CHAPTER 8

Reconstructing Eustatic and Epeirogenic Trends from Paleozoic Continental Flooding Records

Thomas J. Algeo and Kirill B. Seslavinsky

ABSTRACT: Eustatic and epeirogenic trends may be independently quantified given knowledge of flooding patterns for multiple, coexisting, tectonically-independent landmasses. Herein, we develop a method of analyzing paleo-continental flooding records in order to reconstruct both global sea-level trends and individual continental epeirogenic histories. Our method is based on the hypotheses that: 1) co-existing landmasses are likely to have experienced the same range of eustatic fluctuations, 2) differences in flooding are thus primarily a function of differences in coastal hypsometry, and 3) differences in estimated sea-level elevations between individual landmasses and the world may reflect continental epeirogeny. We apply the method to the flooding records of 13 Paleozoic landmasses for which detailed paleogeographic reconstructions are available (Ronov and others, 1984; Khain and Seslavinsky, 1991).

Our analysis indicates that Paleozoic eustatic highstands were probably +100 to +225 m above present sea level, which is substantially lower than previous estimates of +300 m (Vail and others, 1977) to +600 m (Hallam, 1984). Reconstructed epeirogenic histories suggest that Paleozoic continents experienced ±100 m of independent vertical motion relative to global sea level at a 10–40 m.y. timescale. Most large epeirogenic excursions coincided with major tectonic events such as rifting, passive-to-active margin transitions, and continental collisions, and may reflect a range of epeirogenic mechanisms for Paleozoic continents comparable to that documented for modern continents. Close links between eustasy and continental epeirogeny are suggested by the antithetic pattern of Gondwanan crustal motions and global sea-level elevations during the mid-Paleozoic.

1. Introduction

Detailed knowledge of secular changes in global sea-level elevations (eustasy) and broad vertical crustal movements (epeirogeny) is required for thorough understanding of underlying mantle and plate tectonic processes. Although eustasy has been widely regarded as the dominant control on long-term patterns of continental

B. U. Haq (ed.),
Sequence Stratigraphy and Depositional Response to Eustatic, Tectonic and Climatic Forcing, 209–246.

flooding (e.g., Vail and others, 1977; Haq and others, 1987), epeirogeny is now considered to be a factor of equal importance and to respond to the same underlying mantle processes (e.g., Gurnis 1992a,b). In general, eustatic and epeirogenic fluctuations cannot be separated based on stratigraphic data from a single locale, basin, or continent. Isolation of these variables at a sub-continental scale is difficult owing to the flexural rigidity of continental lithosphere and to frequent linkage of the subsidence histories of adjacent sedimentary basins (e.g., Quinlan and Beaumont, 1984; Cloetingh, 1988).

Independent quantification of eustatic and epeirogenic trends may be possible given stratigraphic information from multiple, co-existing, tectonically independent sources. The goals of this contribution are to: 1) develop a method of analysis of the flooding records of co-existing paleo-continents that permits reconstruction of both global sea-level trends and individual continental epeirogenic histories, 2) apply the method to the flooding records of 13 Paleozoic landmasses, and 3) consider the significance of the results of the analysis in relation to documented mechanisms of eustatic and epeirogenic motions.

1.1. Eustasy

Long-term (>10 m.y.) changes in global sea-level elevation are of considerable importance as an expression of variations in mantle convection and heat flow (Turcotte and Burke, 1978; Galer, 1991) and owing to a strong influence on global climate, geochemistry, and biosystems, including greenhouse-icehouse cycles (Fischer, 1984), atmospheric CO_2 levels (Wilkinson and Given, 1986; Berner, 1994), seawater composition and marine carbonate mineralogy (Wilkinson and others, 1985), and biodiversity and mass-extinction patterns (Riding, 1984; Wyatt, 1987). Because many aspects of paleo-mantle behavior and paleo-atmospheric and -oceanic chemistry are difficult or impossible to reconstruct, eustasy has been widely used as a proxy for other variables in global models (e.g., Gaffin, 1987; Galer, 1991).

Despite the obvious importance of and need for accurate information regarding the amplitude of secular eustatic variations, surprisingly little research on long-term eustasy has been undertaken: to date, the only widely-cited Phanerozoic sea-level curves are those of Vail and others (1977) and Hallam (1984). Most extant studies of Paleozoic eustasy are based on sequence stratigraphic or facies analysis of limited geographic areas and have yielded only qualitative trends (e.g., Johnson and others, 1985; Heckel, 1986; Johnson and others, 1991; Schenk, 1991). Quantitative analyses of Paleozoic eustatic trends using well-documented databases are lacking.

1.2. Epeirogeny

Broad (>100 km) vertical crustal motions are potentially of major significance as indicators of mantle-crustal thermal interactions, far-field responses to plate-margin processes, and lithospheric density anomalies associated with melting, intrusion, or phase changes (McGetchin and others, 1980). The epeirogenic his-

TABLE 1
Paleozoic flooding data by continent and epoch*

epoch	age[a]	GOND	PNG	LRNT	LRSS	BALT	SIB	ARM	CHK	KAZ	N-CHN	CHN	S-CHN	IND
LPM	250		15.8[b]									35.7		84.0
EPM	270		18.7									55.7		88.0
LCB	305	16.8			34.6		41.8			20.0		68.5		92.0
ECB	340	12.0			39.4		44.5	76.6		65.7	27.2		63.6	
LDV	370	19.4			41.7		38.1	82.1		57.1	17.0		59.0	
MDV	380	21.1			31.3		45.7	82.1		42.8	12.1		45.4	
EDV	395	27.6			13.4		44.7	75.0		51.5	9.7		50.0	
LSL	415	23.7		17.0		18.1	37.1	75.0	46.6	46.8	11.4			
ESL	430	25.1		28.7		33.7	46.5	84.3	43.3	53.3	28.2			
LOR	445	21.7		60.9		29.8	34.6	80.0	40.0	80.0	6.6			
MOR	465	25.1		41.9		36.3	50.4	83.3	33.3	76.0	70.0			
EOR	490	24.5		41.4		32.4	52.4	76.6	30.0	72.0	73.3			
LCM	515	26.9		47.8		18.1	42.5	60.7	36.6	76.0				
MCM	525	27.2		31.0		29.8	59.4	71.4	33.3	76.0				
ECM	550	24.7		21.0		36.3	72.1	78.5	33.3	68.0				

* Estimates are based on updated versions of the interpretative paleogeographic maps of Khain and Seslavinsky (1991).
[a] Ages of epoch midpoints in Ma.
[b] Fractional flooding of total landmass area in percent for "most-likely" case, $F(ij)_{mean}$.

Uncertainties regarding the original extent of marine strata on continents result from loss of sedimentary rocks through erosion, metamorphism, and deep burial. To allow for uncertainties in flooding estimates, we will bracket our "most likely" value for continent i at epoch j, $F(ij)_{\text{mean}}$, by minimum and maximum estimates of original marine flooding, $F(ij)_{\text{min}}$ and $F(ij)_{\text{max}}$. As the minimum flooding value, we will adopt the area on continent i of extant marine strata of epoch j. Meaningful upper limits on flooding are difficult to establish as these require greater extrapolation beyond available stratigraphic data. For simplicity, we will assume that the potential maximum area of lost marine strata is twice that of our "most-likely" estimate, yielding a maximum flooding value of:

$$F(ij)_{\text{max}} = 2 * F(ij)_{\text{mean}} - F(ij)_{\text{min}}. \quad (1)$$

Estimated values of $F(ij)_{\text{min}}$, $F(ij)_{\text{mean}}$, and $F(ij)_{\text{max}}$ are shown by continent in Fig. 1, and values of $F(ij)_{\text{mean}}$ are tabulated by continent and epoch in Table 1.

2.2. Paleozoic Continental Hypsometry

2.2.1. *Application of Hypsometry to Sea-Level Analysis*

The first step in determining eustatic and epeirogenic trends is to reconstruct paleo-continental hypsometries. The hypsometry of a topographic surface is its cumulative areal frequency with respect to elevation. Continental area-elevation distributions form sigmoidal curves that are convex up at low elevations, concave up at high elevations, and have an inflection point close to sea level (Fig. 2). The slope of a hypsometric curve is the rate of change of elevation with respect to cumulative area for a given elevation or elevation range (Algeo and Wilkinson, 1991). The inflection point of a hypsometric curve represents the elevation at which the slope of the curve is gentlest and, thus, at which the modal areal frequency occurs. The fundamental control on the sigmoidal shape of hypsometric curves is the balance between net continent-interior erosion and net continent-margin deposition. For landmasses in "hypsometric equilibrium", the inflection point is located approximately at the updip margin of coastal-plain wedges at an elevation of several tens of meters above sea level.

Hypsometric curves can be used to convert flooding data to sea-level elevations and to reconstruct secular sea-level trends from a series of paleogeographic maps (Fig. 2). Because the elevation range of Phanerozoic eustatic fluctuations has been within a few hundred meters of present sea level (e.g., Vail and others, 1977; Worsley and others, 1984), only the low-elevation portion of a continental area-elevation distribution ("coastal hypsometry") is of significance for eustatic studies. Flooding data provide information about the hypsometric characteristics of a landmass only within this limited elevation range, and, therefore, reconstruction of paleo-continental hypsometries is constrained to the same range of elevations. As a first approximation, we assume that paleo-continental hypsometries within the elevation range of interest are linear. Although modern continental hypsometries are strongly non-linear over elevation ranges of several kilometers (Harrison and others, 1983), deviations from linearity are small within a few hundred meters of present sea level, and this is likely to have been valid for paleo-continents as well.

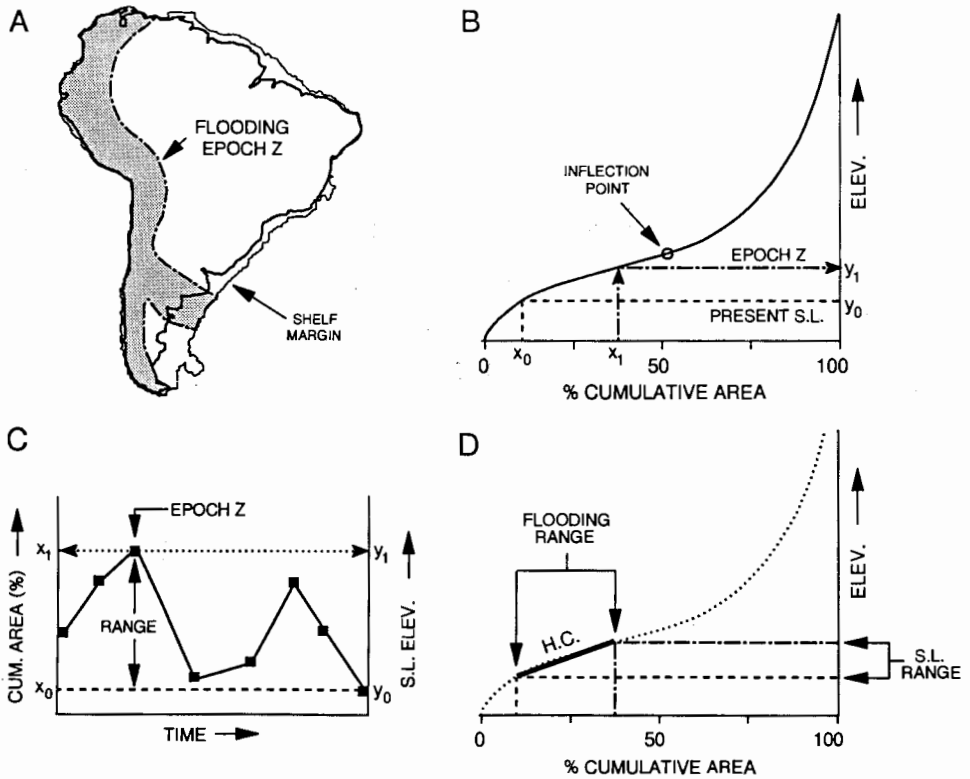

Fig. 2. Example of calculation of sea-level elevations using hypsometry and continental flooding data. (A) Area flooded for a given epoch is measured from an equal-area paleogeographic map relative to a specified reference level, such as the shelf margin. (B) Fractional area flooded (x_1) is converted to sea-level elevation (y_1) using a landmass-specific hypsometric curve. (C) Secular sea-level variation curve is constructed from a series of paleogeographic maps. (D) Given time-invariant continental coastal hypsometry, a specified flooding range yields a corresponding range of sea-level elevations. A "hypsometric chord" (H.C.) is a linear representation of part of a continental area-elevation distribution.

We term linear segments of continental area-elevation distributions "hypsometric chords" (Fig. 2D).

The principal difficulty in using hypsometry for eustatic analysis is in selecting an appropriate hypsometric curve with which to transform ancient flooding records to sea-level elevations. Because paleo-continental hypsometries cannot be reconstructed on purely theoretical grounds, modern area-elevation distributions must be utilized as analogs. However, continental hypsometries change through time, and, consequently, modern area-elevation distributions are likely to yield increasingly less accurate sea-level estimates for progressively older flooding records (Algeo and Wilkinson, 1991). This limitation has constrained previous hypso-

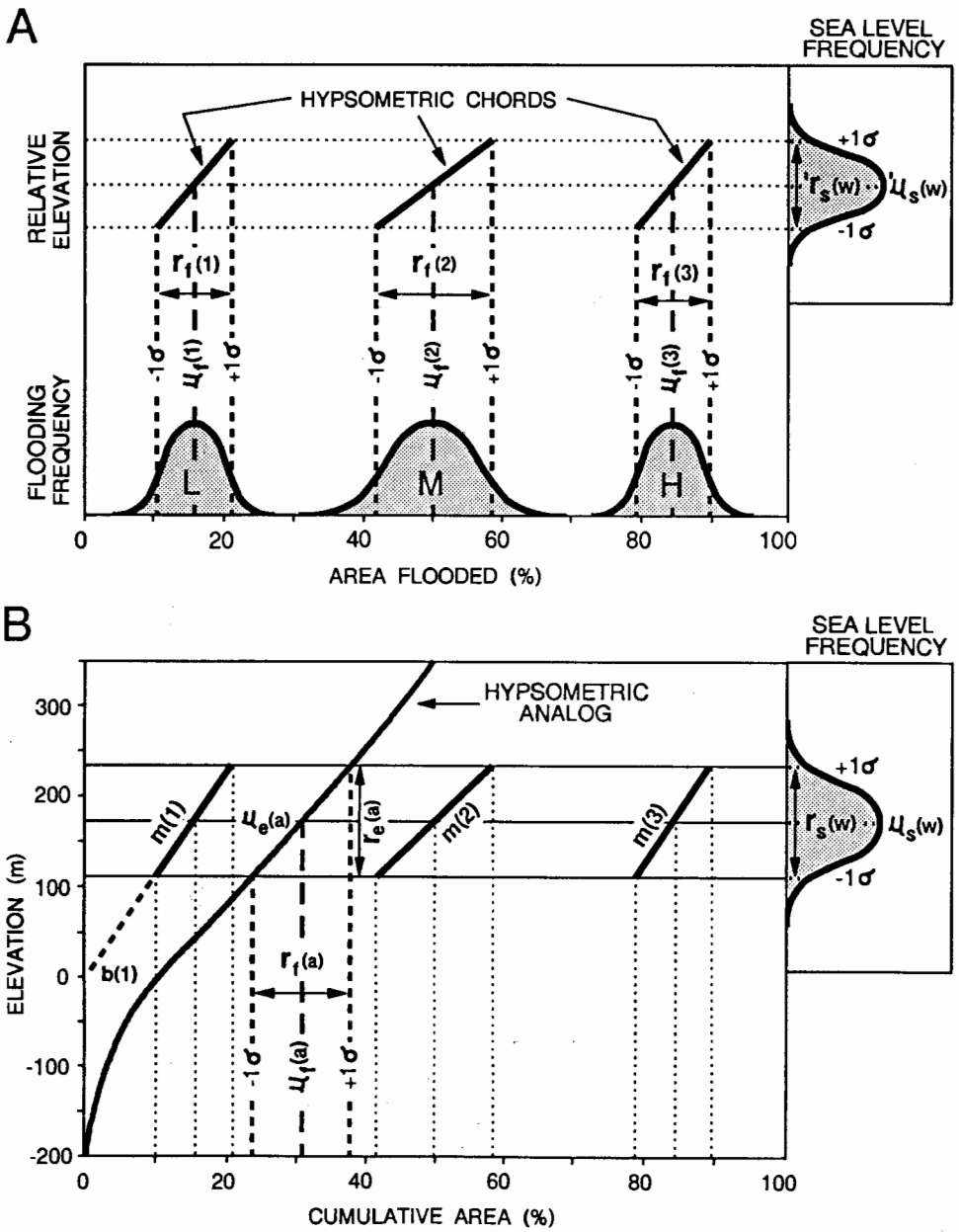

Fig. 3. Reconstruction of paleo-continental hypsometric chords. (A) Relative (non-dimensional) scaling of hypsometric chords for three co-existing landmasses exhibiting low (L), medium (M), and high (H) degrees of average flooding, $\mu_F(i)$, and variable flooding ranges, $\mu_F(i) + \sigma_F(i)$ (bottom). As co-existing landmasses experience the same mean and range of eustatic elevations (upper right), differences in means and ranges of flooding values among continents record differences in their coastal hypsometries (top). (B) Absolute scaling of hypsometric-chord elevations using a modern hypsometric analog, for which an "expected" range of flooding is estimated. Actual elevation range is dependent on choice of analog.

TABLE 2
Flooding ranges for Paleozoic continents

	Mean[a]	Min.[a]	Max.[a]
Gondwana	22.8±4.3[b]	16.3±3.8	29.3±6.1
Pangea	17.3±1.4	14.3±1.2	20.3±1.7
Laurentia	36.2±13.6	32.4±13.9	40.1±13.5
Laurussia	32.1±10.0	29.2±10.0	35.0±10.1
Baltica	29.3±6.8	28.0±6.7	30.8±7.0
Siberia	46.9±9.6	42.7±9.0	51.2±10.9
Armorica	77.1±6.2	61.3±10.5	92.0±7.6
Chukotka	37.0±5.3	16.7±5.0	57.5±6.4
Kazakstania	60.4±16.6	53.5±16.3	67.4±17.5
North China	28.4±24.1	25.8±24.3	31.0±24.0
China (united)	53.3±13.5	50.5±12.8	56.2±14.3
South China	54.5±7.1	44.3±5.9	64.8±8.7
Indochina	88.0±3.2	48.0±5.7	100.0±0.0

[a] Means and standard deviations of flooding values for each continent, $\mu_F(i) \pm \sigma_F(i)$, based on values of $F(ij)_{mean}$, $F(ij)_{min}$, and $F(ij)_{max}$, respectively.
[b] Fractional flooding of total landmass area in percent.

flooding values should be recorded for a group of paleo-continents. Differences in the mean, standard deviation, and range of flooding values for each landmass can be used to partially reconstruct a characteristic long-term mean coastal hypsometry for each landmass (Fig. 3A). Hypsometric reconstruction proceeds in two steps: 1) non-dimensional scaling of paleo-continental hypsometric chords, and 2) absolute scaling of hypsometric chords using a modern continental analog. In the first step, the means and ranges of flooding values for each paleo-continent are set equal to the same non-dimensional mean and range of eustatic elevations, $'\mu_S(w)$ and $'r_S(w)$ (Fig. 3A). In the second step, dimensional values of the mean and range of eustatic elevations, $\mu_S(w)$ and $r_S(w)$, are substituted for $'\mu_S(w)$ and $'r_S(w)$, permitting calculation of dimensional values for the slopes and y-intercepts of paleo-continental hypsometric chords:

$$m(i) = r_S(w)/r_F(i), \tag{5}$$

$$b(i) = \mu_S(w) - m(i) \cdot \mu_F(i), \tag{6}$$

h ( ) d $b(\cdot)$ the slope a d y ntercept of the hypsometric chord of
S

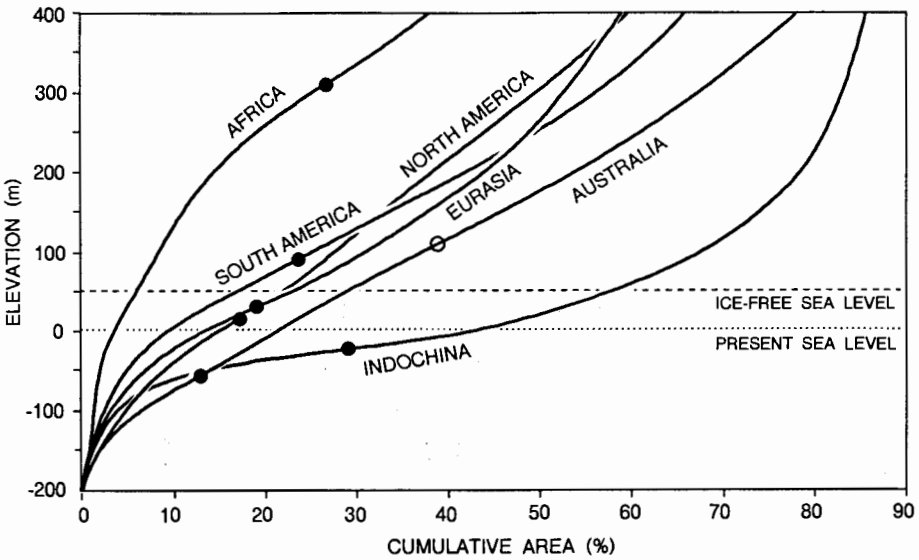

Fig. 4. Coastal hypsometries of modern continents (excluding Antarctica) with respect to shelf margins (ca. −200 m). Hypsometric curves are cubic-splined versions of the area-elevation data of Harrison and others (1983). The modern Indochina curve was calculated from equal-area 1:2,500,000 topographic maps and includes Borneo, Sumatra, Java, the Malaysian peninsula, the Southeast Asian peninsula (northward to the Song Ma-Red River region in northern Vietnam and westward to the Sagaing Fault zone in central Burma; Hutchison, 1989), and all intervening shallow-marine areas (≥ -200 m). Inflection points (I, in meters; circles) and hypsometric-slope minima (m, in meters/%area) for Eurasia: $I = 30$, $m = 5.0$, Africa: $I = 310$, $m = 6.7$; North America: $I = 15$, $m = 6.7$; South America: $I = 90$, $m = 5.6$; Australia: $I = -60, +110$, $m = 6.1$, 5.6; and Indochina: $I = -25$, $m = 1.4$. Modern Indochina is included to illustrate the range of potential hypsometric variation; it may be a better analog for small Paleozoic landmasses than modern continents.

Choice of Modern Hypsometric Analog. As our analytical method only permits reconstruction of *relative* coastal hypsometries based on paleo-continental flooding data, development of an *absolute* elevation scale requires recourse to a modern hypsometric analog. Next, we consider the hypsometric characteristics of modern continents, evaluating their suitability as hypsometric analogs. The best compilation of modern area-elevation data is that of Harrison and others (1983), who utilized a Defense Mapping Agency database consisting of global elevation values for 1 degree squares at elevation intervals of 100 m. We have fitted the area-elevation data of Harrison and others with cubic splines to produce coastal hypsometric curves for each modern continent (Fig. 4).

The curves for North America, South America, and Eurasia are rather similar, having hypsometric slope minima of 5.0 to 6.7 m/%area and inflection-point elevations slightly above present sea level (+15 m to +90 m; Fig. 4). For reasons discussed below, these continents are probably close to their long-term hypsometric equilibria. Although Africa and Australia have similar hypsometric slope minima

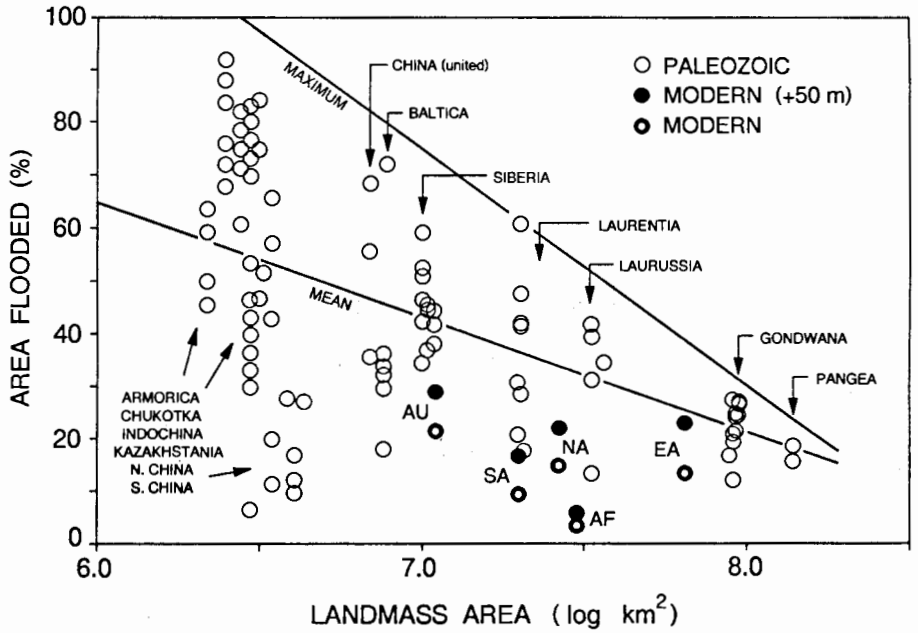

Fig. 5. Flooding versus landmass area for Paleozoic and modern continents. For Paleozoic continents, mean and maximum flooding decrease with increasing landmass area. For modern continents, flooding values are shown with respect to both present sea level (circles with dots) and that of an ice-free modern world (+50 m above present sea level; solid circles). Modern continents: AU = Australia, SA = South America, NA = North America, AF = Africa, and EA = Eurasia. Note that modern continents exhibit generally low degrees of flooding in relation to Paleozoic landmasses of equivalent area.

(Fig. 7A), and a mean elevation of +160 m and an elevation range of 96–224 m based on the American analog (Fig. 7B). Although the hypsometries of Eurasia and North and South America are similar (Fig. 4), the two analogs yield large differences in estimated elevation ranges owing to differences in the degree to which the actual flooding of modern continents diverges from their "expected" Paleozoic flooding values: present flooding of Eurasia (23%; Fig. 5) is close to its expected Paleozoic mean (25%; Fig. 6A), but present flooding of America (22%) is considerably lower than its expected mean (35%). This makes clear the implications of choosing Eurasia versus America as a hypsometric analog: the former implies that modern sea-level elevations are rather typical for the Phanerozoic as a whole, whereas the latter implies that they are unusually low.

2.3. Paleozoic Sea-Level and Epeirogenic Trends

2.3.1. Calculation of Sea-Level Elevations

Once coastal hypsometric chords have been constructed and scaled for individual Paleozoic landmasses (Fig. 7), calculation of sea-level elevations for each continent

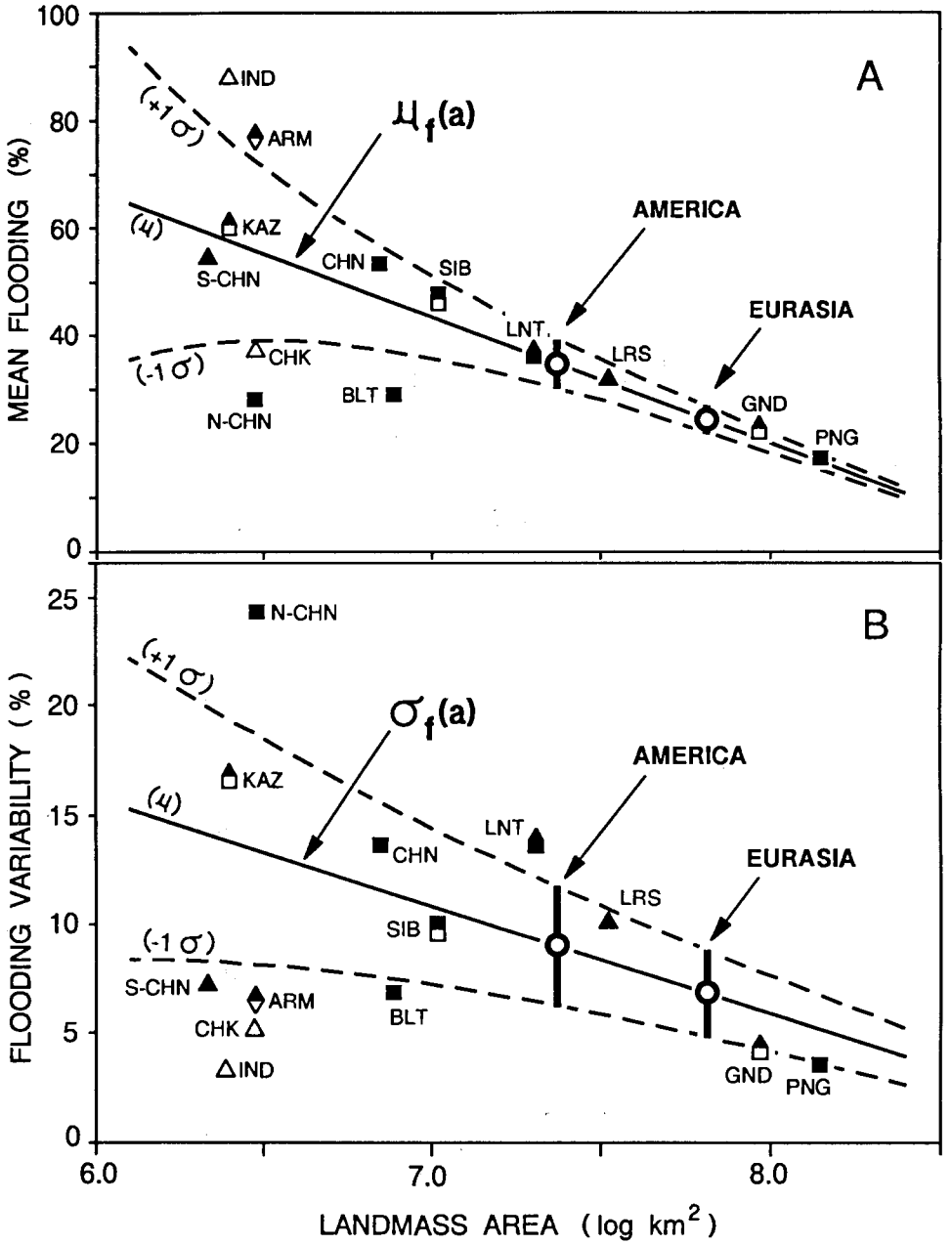

Fig. 6. Mean flooding and flooding variability for Paleozoic continents. Both (A) mean flooding, $\mu_F(i)$, and (B) flooding variability, $\sigma_F(i)$, decrease and exhibit a narrower range with increasing landmass area. These relationships are used to estimate "expected" means and ranges of flooding values for hypsometric analogs. Paleozoic continents equivalent in area to modern Eurasia and America would exhibit flooding ranges of 25 ± 7% and 35 ± 9%, respectively (open circles). Uncertainties in estimates of "expected" mean flooding and flooding variability (solid vertical bars) are based on ±1 regression lines (dashed). The low flooding variabilities exhibited by some small paleo-continents (e.g., Chukotka) reflect time-invariant flooding estimates that result from a lack of detailed stratigraphic information rather than from genuinely small ranges of flooding values.

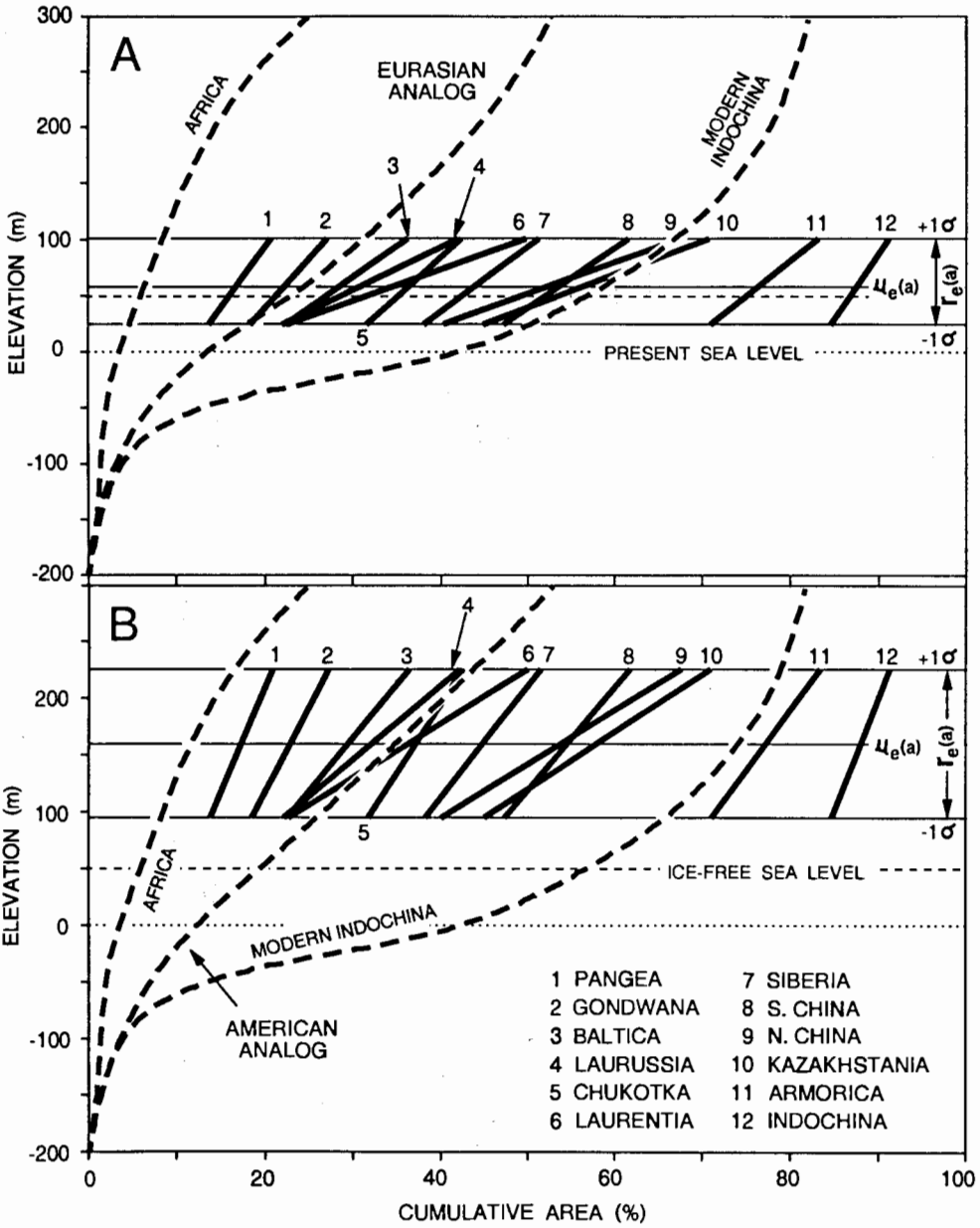

Fig. 7. Scaled hypsometric chords of Paleozoic continents using Eurasian (A) and American (B) analogs. The Eurasian model yields a mean elevation of +60 m and an elevation range of 24–102 m, whereas the American model yields a mean elevation of +160 m and an elevation range of 96–224 m. The area-elevation curves of modern Africa and Indochina bracket the coastal hypsometries of most Paleozoic continents. Note that choice of an American analog implies steeper paleo-continental hypsometries and higher sea-level elevations than choice of a Eurasian analog.

at each epoch is possible (Figs. 2, 8). This involves conversion of flooding values to sea-level elevations using the characteristic hypsometric chord of each paleo-continent:

$$S(ij) = m(i) \cdot F(ij) + b(i), \tag{7}$$

where $S(ij)$ is the sea-level elevation estimate for continent i at epoch j. For example, Laurentia has flooding values of 21%, 32%, and 48% for the Lower, Middle, and Upper Cambrian, respectively (Table 1), yielding sea-level elevations of 20 m, 45 m, and 90 m based on the Eurasian analog, or 80 m, 130 m, and 220 m based on the American analog (Figs. 7, 8). Sea-level elevation estimates are not appreciably affected by use of linear hypsometric "chords" rather than continuously varying curves, because most modern continents have fairly uniform hypsometric slopes at low elevations (Fig. 4). Significant non-linearity would develop only at extreme flooding values (i.e., $> +2\sigma$).

Once continental sea-level elevations have been determined for each epoch, global sea-level elevations may be calculated by several methods. In theory, each paleo-continent is an independent recorder of eustasy having equal validity, and, therefore, global sea-level elevations could be calculated as a simple unweighted average of individual continental sea-level elevations for each epoch:

$$S(wj) = i \sum_{1}^{m} S(ij)/m, \tag{8}$$

where $S(wj)$ is the unweighted estimate of global sea-level elevation, and m is the number of continents extant during epoch j. However, the variance of individual continental sea-level estimates is related to flooding data quality: on average, estimates based on excellent- to good-quality data deviate by 40–45 m from global mean sea-level elevations, whereas those based on poor-quality data deviate by 62 m. Therefore, we prefer eustatic estimates reflecting data quality:

$$\underline{S}(wj) = i \sum_{1}^{m} [S(ij) \cdot Q(ij)] / i \sum_{1}^{m} Q(ij), \tag{9}$$

where $\underline{S}(wj)$ is the quality-weighted estimate of global sea-level elevation, and $Q(ij)$ is the quality value of the flooding estimate for continent i at epoch j. Quality values were assigned to individual continental sea-level estimates according to a scale of 1.0 for excellent-, 0.5 for good-, 0.33 for fair-, and 0.125 for poor-quality flooding data (quality values based on ratios of flooding extrapolation values; see above). Global sea-level trends for quality-weighted estimates are shown in Fig. 9.

2.3.2. *Calculation of Epeirogenic Trends*

Individual continental sea-level estimates diverge to greater or lesser degrees from the global mean elevation for each epoch, yielding "elevation residuals":

$$\Theta S(ij) = S(ij) - S(wj), \tag{10}$$

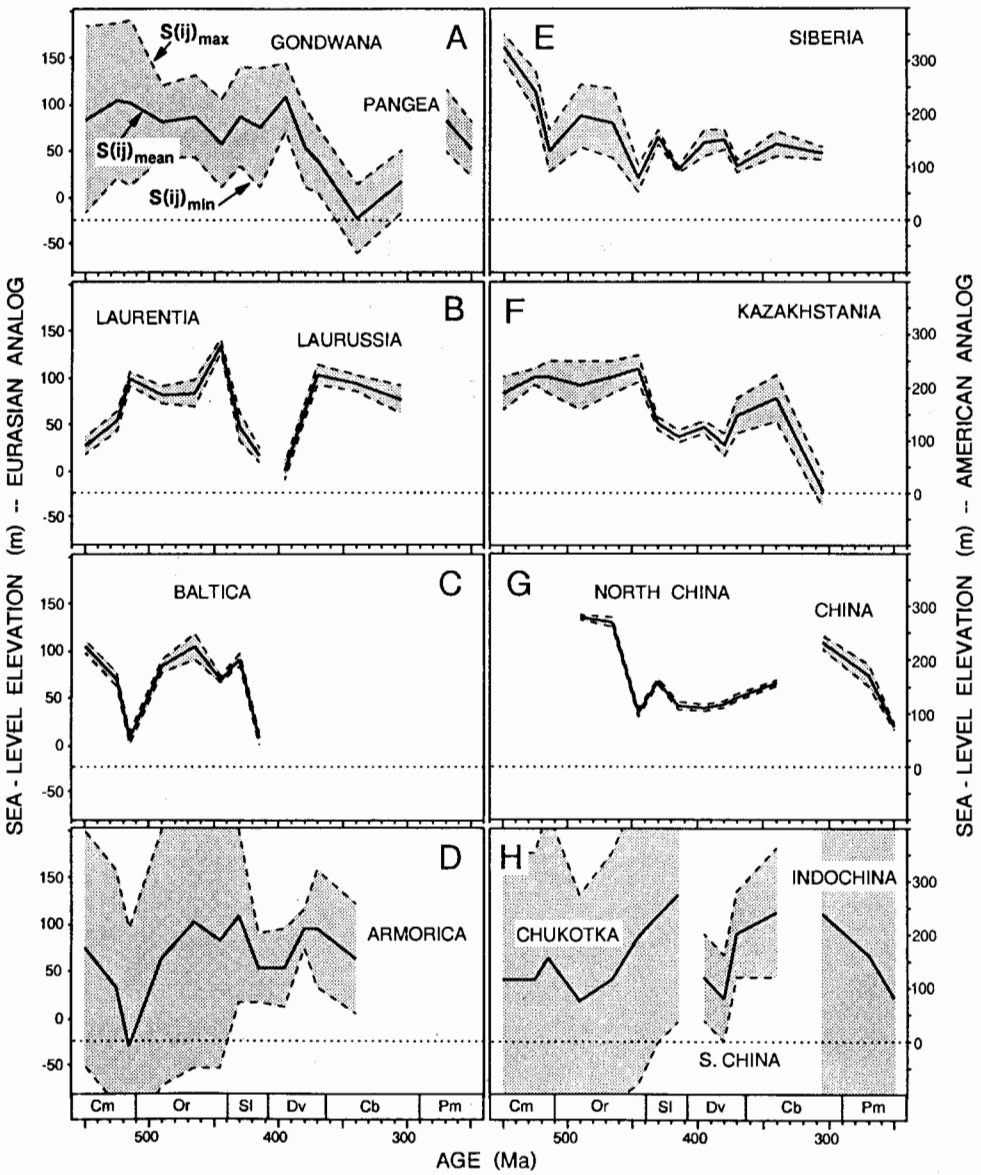

Fig. 8. Sea-level elevations for individual Paleozoic continents. Estimates are based on the "most-likely" or mean flooded area ($F(ij)_{mean}$; solid line) and on minimum and maximum flooding estimates ($F(ij)_{min}$ and $F(ij)_{max}$, respectively; dashed lines). Sea-level trends are significant where elevation changes exceed the uncertainty range. Elevation scales are shown for both Eurasian (left) and American (right) analogs.

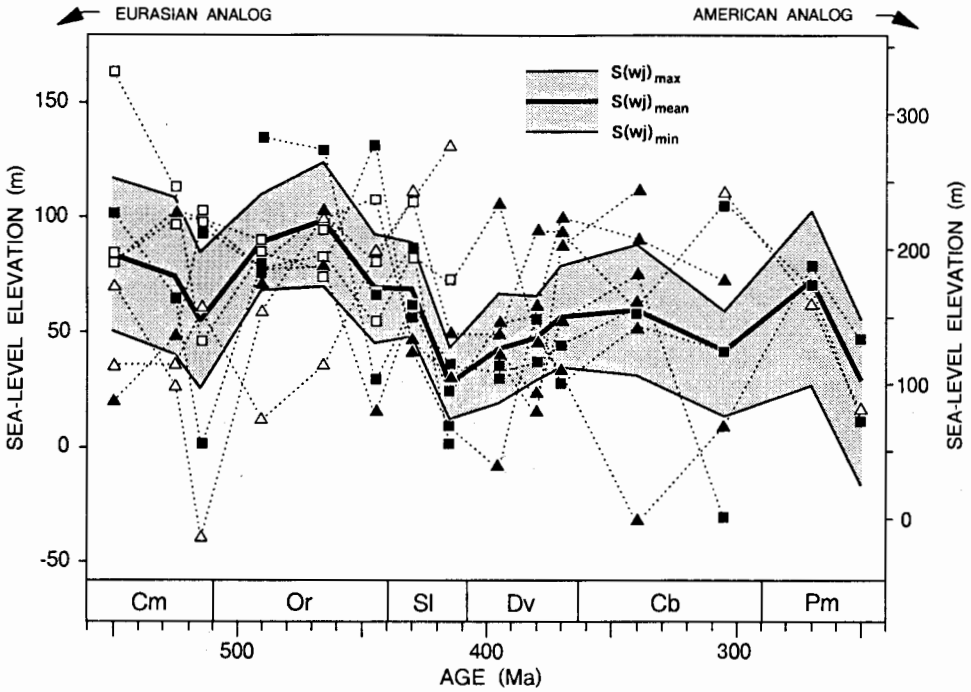

Fig. 9. Global and stacked continental sea-level elevations for the Paleozoic. Symbols on continental sea-level curves (dotted) represent data quality; refer to Fig. 1 for meaning of symbols and to Fig. 8 for identification of paleo-continents. The mean global curve (heavy solid line) is a quality-weighted average of continental sea-level elevations using weights of 1.0 for excellent (solid squares), 0.5 for good (solid triangles), 0.33 for fair (open squares), and 0.125 for poor data (open triangles). The uncertainty range for global sea-level elevations (shaded) is based on minimum and maximum flooding values for all paleo-continents at each epoch (Fig. 1). Elevation scales are shown for both Eurasian (left) and American (right) analogs.

where $\Theta S(ij)$ is the difference between the sea-level estimate for continent i and the global mean at epoch j. Generally, high (low) flooding values (Fig. 1) yield positive (negative) elevation residuals (Fig. 10). The maximum amplitudes of elevation residuals are about +90 m and +150 m based on the Eurasian and American analogs, respectively, which are comparable in magnitude to eustatic ranges of ca. 100 m and 225 m for the respective hypsometric analogs (Fig. 9).

Deviations of continental sea-level estimates from the global mean are due to one of two causes: 1) secular changes in paleo-continental hypsometry, or 2) errors in flooding estimates. Although we have assumed to this point that the coastal hypsometry of each Paleozoic landmass is time-invariant, secular changes in the elevation or slope of a hypsometric chord would result in deviations of continental sea-level elevations from the global mean. The simplest interpretation of elevation residuals in terms of secular hypsometric variation invokes vertical displacement of hypsometric chords such that a positive (negative) motion yields a negative (positive) elevation residual of equal magnitude. This interpretation

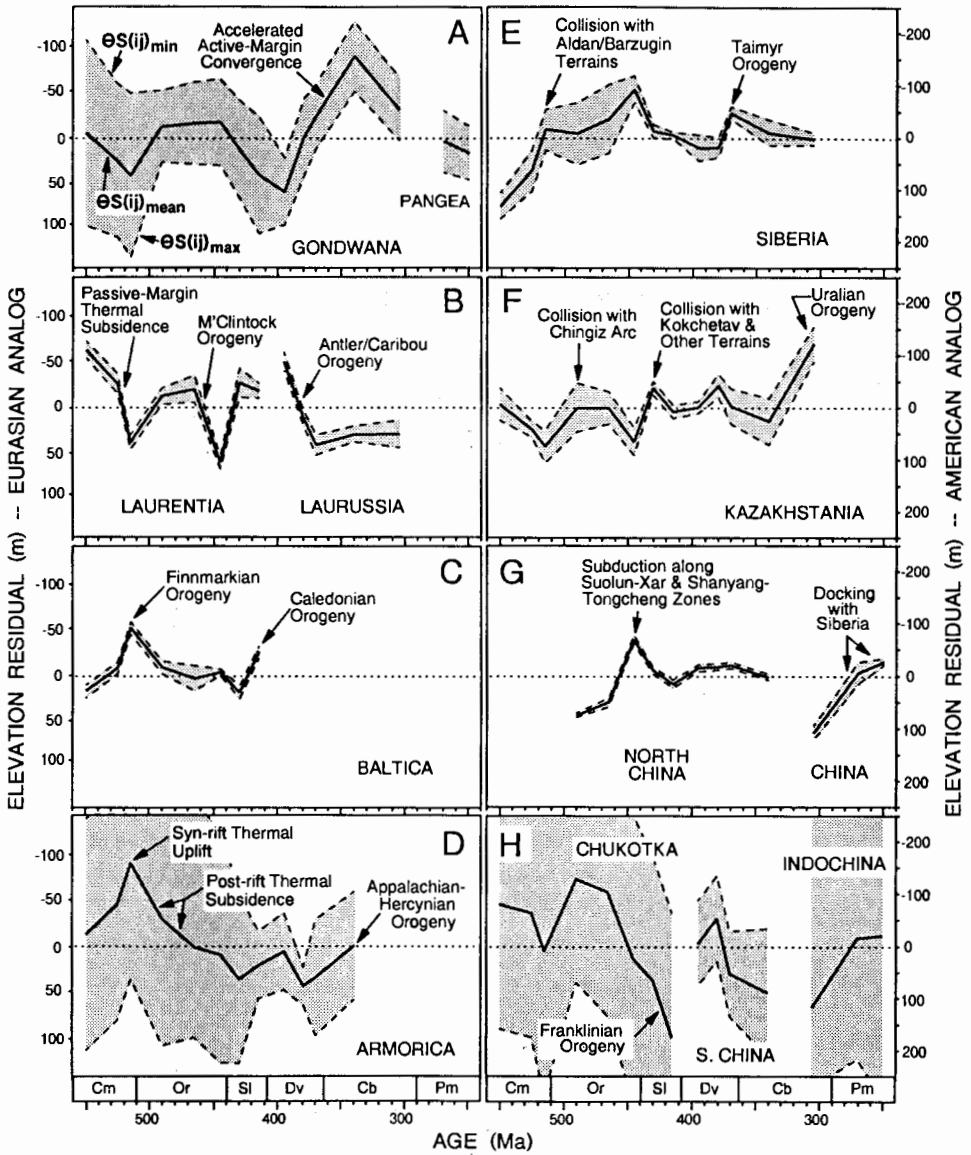

Fig. 10. Elevation residuals for individual Paleozoic continents. An elevation residual is the deviation of a continental sea-level estimate from the global mean at a given epoch (Fig. 9). Residuals represent a combination of errors in flooding estimates and secular changes in paleo-continental hypsometry, e.g., as a consequence of epeirogeny. To facilitate interpretation of residuals as epeirogenic motions, elevation scales are inverted: a negative residual (low relative sea level; Fig. 8) is equivalent to positive epeirogenic motion (uplift) and, conversely, a positive residual (high relative sea level) is equivalent to negative epeirogenic motion (subsidence). If viewed as vertical movement about a fixed, neutral level of buoyancy, these curves yield an "epeirogenic history" for each landmass. Uncertainty ranges for elevation residuals (shaded) are based on minimum and maximum flooding values (Fig. 1). Elevation scales are shown for both Eurasian (left) and American (right) hypsometric analogs; values cited in text are for the American analog.

receives empirical support from modern continental hypsometric anomalies (e.g., Africa and Australia; Fig. 4), in which the sense and scale of offset of hypsometric inflection points is consistent with the direction and relative magnitude of recent vertical crustal motions.

Alternatively, elevation residuals may result in part or in whole from errors in flooding estimates (Fig. 1). The potential effects of such errors may be evaluated by calculating an uncertainty range for elevation residuals: by substituting $F(ij)_{max}$ and $F(ij)_{min}$ for $F(ij)_{mean}$ in Eq. (10), upper ($\Theta S(ij)_{max}$) and lower ($\Theta S(ij)_{min}$) limits on elevation residuals for continent i at epoch j are established (dashed lines, Fig. 10). When the uncertainty range encompasses the origin of the ordinate (i.e., 0 m), the difference between individual continental and global mean sea-level estimates is probably not significant (e.g., Cambro-Silurian, Gondwana; Fig. 10A). When elevation residuals are larger than the enclosing uncertainty envelope, they are likely to represent secular changes in paleo-continental coastal hypsometries (e.g., Cambro-Silurian, Laurentia; Fig. 10B).

3. Discussion

3.1. Eustasy

3.1.1. Paleozoic Eustatic Elevations

First-order Paleozoic eustatic trends are similar in our curve and those of Vail and others (1977) and Hallam (1984), all of which exhibit a Cambro-Silurian Caledonian and a Devono-Permian Appalachian-Hercynian cycle (Fig. 11). On the other hand, these curves exhibit large differences with regard to eustatic amplitudes: the Vail and Hallam curves have Paleozoic sea-level maxima of +200 m to +300 m and +300 m to +600 m, respectively, which are substantially higher than those of this study (+100 m to +225 m). Independent estimates of Paleozoic eustatic amplitudes are few. Backstripping methods of subsidence analysis have yielded "changes in accommodation" (eustasy plus local tectonism) of ca. 100–200 m in the North American midcontinent area during major Paleozoic transgressions (e.g., Bond and Kominz, 1991), although such estimates may exceed 300 m for continental margin sequences (Osleger and Read, 1993).

A comparison of the Paleozoic supercycle with the better documented Mesozoic–Cenozoic supercycle is warranted. The Late Cretaceous highstand has been estimated at +175 m to +250 m based on hypsometry, mid-ocean ridge volume analysis, sequence stratigraphy, and subduction rate analysis (e.g., Bond, 1979; Harrison and others, 1983; Kominz, 1984; Haq and others, 1987; Engebretson and others, 1992), which is lower than the Paleozoic highstand elevations of Vail and others (1977) but higher than those of this study. Further, the total length of passive margins created during supercontinent breakup was greater during the Jurassic-Cretaceous (ca. 35,000 km; Harrison and others, 1981; Heller and Angevine, 1985) than during the Eocambrian (ca. 18,000 km; Bond and others, 1984). Because passive-margin lengths and eustatic elevations are both controlled by geotectonic supercycles (e.g., Heller and Angevine, 1985; Gurnis, 1992a), inferred positive co-

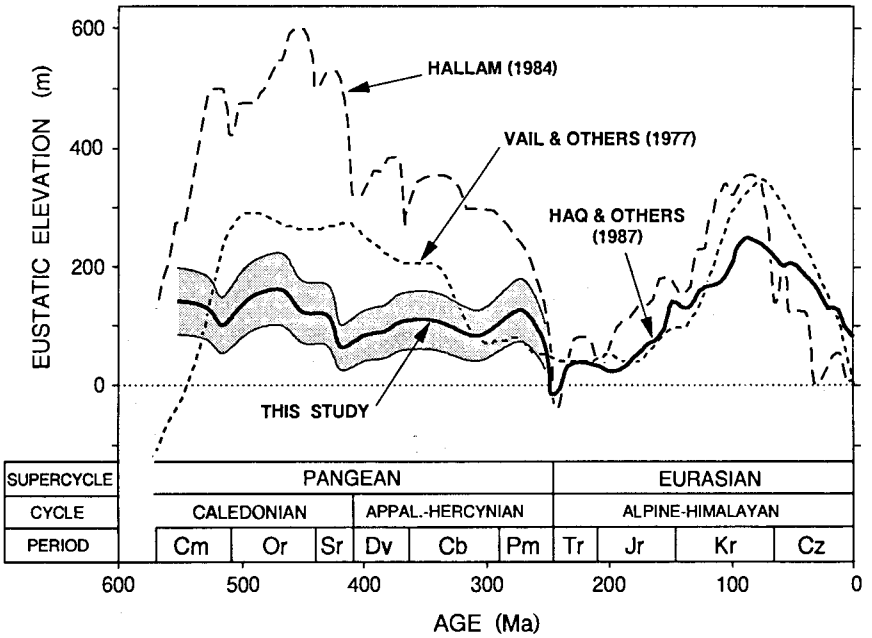

Fig. 11. Phanerozoic eustatic trends according to Vail and others (1977), Hallam (1984), Haq and others (1987; smoothed version of their long-term curve), and this study. Our Paleozoic curve (heavy solid line; spliced to Haq curve at Permo-Triassic boundary) is based on mean values for all model parameters and a hypsometric analog that is an unweighted average of the Eurasian and American curves; uncertainty range (shaded) from Fig. 9. Note the substantially lower Paleozoic eustatic elevations of our curve relative to those of the two existing Phanerozoic sea-level curves.

variance between these parameters implies that eustatic elevations associated with the Paleozoic were no greater than those of the Mesozoic–Cenozoic supercycle.

3.1.2. Controls on Long-Term Eustasy

Although many factors influence eustasy (e.g., Donovan and Jones, 1979; Harrison, 1988), long-term (i.e., > 10 m.y.) sea-level cycles are commonly attributed to changes in the lengths and spreading rates of mid-ocean ridges (MORs; Pitman, 1978; Kominz, 1984; Larson, 1991) or to interbasinal differences in the age distribution of oceanic lithosphere (Heller and Angevine, 1985). The potential effects of these factors on global sea-level elevations are substantial: two-fold reduction of global spreading rates since the Late Cretaceous may have caused a eustatic fall of ca. 230 ± 115 m (Kominz, 1984), and evolution of ocean-crust age distributions during growth of an Atlantic-type ocean basin may induce eustatic fluctuations of ca. 40–100 m (Heller and Angevine, 1985). A related factor linked to geotectonic cycles is ocean basin volume, which decreases during continental rifting and attenuation of passive margins and increases during continental collision and lithospheric thickening in orogens. The potential effects of this factor are substantial: Heller and Angevine (1985) estimated a 50-90 m eustatic rise owing to continen-

tal margin extension during development of an Atlantic-type ocean, and Harrison (1988) estimated a 70-m eustatic rise associated with post-Jurassic passive-margin creation and a 20-m eustatic fall associated with the Eocene-to-Recent collision of India and Eurasia.

The largest changes in Paleozoic eustatic elevations are associated with the onset and termination of geotectonic supercycles. A rise of 50–100 m during the Early–Middle Ordovician (Figs. 9, 11) may reflect a combination of increases in MOR lengths and spreading rates, formation of new Atlantic-type ocean basins, and decreases in ocean basin volume associated with attenuated passive margins. During geotectonic rift phases, all three factors operate to raise global sea levels, as during the Jurassic-Cretaceous disintegration of Pangea (Heller and Angevine, 1985; Wyatt, 1986). Absence of information regarding lengths and spreading rates of Paleozoic MORs precludes determination of the relative contribution of each factor to the Early–Middle Ordovician eustatic highstand (e.g., Vail and others, 1977; Hallam, 1984; this study). However, the timing of the Early Paleozoic highstand is consistent with peak sea-level elevations some 50–100 m.y. after supercontinent breakup in response to shifts in the area–age distribution of oceanic lithosphere (e.g., Heller and Angevine, 1985).

The Caledonian and Appalachian–Hercynian cycles are terminated by eustatic falls of 40–70 m during the Late Silurian and Late Permian, respectively (Figs. 9, 11), which coincide with major continental collisions, i.e., Late Silurian suturing of Laurentia, Baltica, and Chukotka to form Laurussia, and Late Carboniferous-Permian suturing of Gondwana, Laurussia, Kazakhstania, and Siberia to form Pangea. Several mechanisms could account for synchroneity of major Paleozoic eustatic falls with continental collision events, although some explanations (e.g., reduced global spreading rates) lack empirical support. The simplest explanation is an increase in ocean basin volume resulting from orogenic thickening of continental lithosphere during the Caledonian and Appalachian/Hercynian/Uralian orogenies, similar to but larger than that proposed for the India–Eurasia collision (Harrison, 1988).

3.2. Continental Epeirogeny

Paleozoic continental elevation residuals (Fig. 10) may record epeirogenic motions, as suggested by large-scale vertical displacements of modern continents (e.g., Fig. 4). Given the limited existing data on continental epeirogenic histories (Bond, 1976, 1978a,b, 1979; Harrison and others, 1981, 1983; Hallam, 1984; Veevers, 1984; Harrison, 1988, 1990), these residuals represent a potentially valuable source of information regarding the frequency, magnitude, and origin of continental crustal motions. However, interpretation of paleo-continental elevation residuals requires a thorough understanding of epeirogenic processes. Therefore, before proceeding to consider the significance of Paleozoic elevation residuals, we begin with a review of the Cretaceous-Cenozoic epeirogenic histories of modern continents and of proposed underlying mechanisms.

3.2.1. *Modern Continental Epeirogeny*

Complex patterns of crustal uplift and subsidence have been documented for most modern continents during the Cretaceous and Cenozoic. In Africa, uplifts occur as broad plateaus (ca. 10^6 km^2) up to 1 km in height with local domes (ca. 10^5 km^2) greater than 3 km in height (Sahagian, 1988; Westaway, 1993). Domes exhibit complex Tertiary uplift histories with distinct phases of ca. 2–10 m.y. duration (King, 1962; Rosendahl, 1987; Sahagian, 1988). In Australia, the most prominent long-wavelength crustal feature is a north-south depression through the center of the continent, transecting the Simpson Desert, Euroka Arch, and Gulf of Carpentaria, and continuing southward at least as far as the Southeast Indian Ridge, where it is known as the Australian-Antarctic Discordance (AAD; Palmer and others, 1993).

Elsewhere, broad crustal uplifts are mostly associated with Late Cretaceous and younger orogenies. In Asia, the Tibetan Plateau has been uplifted 4–5 km in response to the collision of India with Eurasia (Molnar, 1989; Harrison and others, 1992). In North America, large areas of the West, including the Basin and Range, Cordillera, Colorado Plateau, and western Great Plains, have been uplifted by 1–3 km during the Late Cretaceous–Recent Laramide Orogeny (Bond, 1979; Sahagian, 1987; Ruddiman and others, 1989). Recent broad uplift has occurred in central and southern Europe in association with the Alpine–Carpathian and Pyrennean orogenies (Bond, 1979), as well as in the Andean Altiplano of South America (Allmendinger, 1986). On the other hand, broad areas of the Russian Platform may have subsided (Bond, 1979) or maintained a stable elevation since the Cenomanian (Sahagian, 1989). Thus, all modern continents appear to have been affected to varying degrees by recent epeirogenic motions.

Hypsometric analysis is capable of identifying major epeirogenic events. However, because this method integrates elevations over the surface of an entire continent, hypsometric estimates of elevation changes for a given event are invariably muted in relation to actual crustal displacements occurring at a subcontinental scale. Thus, although large areas of eastern Africa and western North America have experienced uplift of 1–3 km during the Cenozoic, Bond's (1978b) analysis identified an average (continent-scale) uplift of 210 m for Africa (Oligocene–Recent) and an average uplift of 150 m for North America (Paleocene–Eocene). Thus, it must be recognized that hypsometric estimates of average continent-scale elevation changes do not represent the actual length scales of epeirogenic events.

3.2.2. *Mechanisms of Modern Continental Epeirogeny*

Although the phenomenon of epeirogeny is well documented, large uncertainties exist regarding the operation and relative importance of various causative factors. Three broad categories of mechanisms have been proposed: thermal isostatic, non-thermal isostatic, and dynamic (i.e., non-isostatic; Table 3). Each mechanism exhibits characteristic lateral, vertical, and temporal scales of operation. The lateral scale of epeirogenic motions is definitionally delimited to $> 10^2$ km (shorter flexural wavelengths are characteristic of local tectonic processes) and is controlled by the rheology of continental lithosphere and the size and locus (i.e., supra-, intra-,

or subcrustal) of applied forces (Forsyth, 1985). Vertical crustal displacements range from a few meters to a few kilometers, and characteristic timescales range from 10^3 yr to 10^8 yr (Table 3).

Among the numerous proposed mechanisms of continental epeirogeny (Table 3), some are more thoroughly documented than others. In this section, we consider several epeirogenic mechanisms in greater detail, focusing on those that: 1) have well-documented examples, and 2) operate at length and time scales large enough to permit recognition through hypsometric analysis, and 3) are linked to tectonic processes for which independent geologic evidence may be available:

1) *Thermal subsidence of rift margins.* Conductive and advective cooling of attenuated passive margins following rifting results in exponentially-declining subsidence of 2–3 km, often amplified substantially owing to sediment loading (Steckler and Watts, 1978; Royden and others, 1980). Characteristic features of this process are hinged subsidence of long, linear belts along young passive margins. Examples include the Paleozoic (Bond and others, 1989; Osleger and Read, 1993) and Mesozoic-Cenozoic passive margins of North America (Steckler and Watts, 1978; Heller and others, 1982).

2) *Mantle plumes.* Thermal buoyancy, in conjunction with dynamic mantle upwelling, results in uplift of continental lithosphere by 1–3 km over mantle plumes. Characteristic features of this process are small domical uplifts within broad plateaus and association with tensional stress regimes, alkaline magmatism, and continental fragmentation. Examples include Mesozoic West Gondwana (White and McKenzie, 1989; Peate and others, 1990) and late Cenozoic East Africa (Sahagian, 1988; Westaway, 1993).

3) *Dynamic topography.* Thermal/density anomalies of mantle convective origin result in broad topographic and geoid anomalies (Hager and others, 1985; Gurnis, 1990b). The largest anomalies are associated with low-degree patterns of mantle convection: highs over mantle upwelling zones and lows over mantle downwelling zones. Because continents tend to move away from the former and toward the latter, long-term cycles of continental flooding may be linked to drift with respect to dynamic topography (Gurnis, 1988). Examples include Africa, which is probably located over a mantle upwelling zone (Hager and others, 1985), and Australia, which may straddle a mantle downwelling zone, as suggested by seismic, gravimetric, and geochemical data (Sempéré and others, 1991; Pyle and others, 1992; Kuo, 1993; Palmer and others, 1993).

4) *Variations in intraplate stress fields.* Changes in the horizontal forces acting on a plate cause changes in lithospheric density, leading to uplift under tensional stress regimes and subsidence under compressional ones (Gay, 1980; Cloetingh, 1988; Cathles and Hallam, 1991). A characteristic feature of this process may be episodes of linked subsidence in intracratonic basins lacking an obvious tectonic or eustatic driver. Possible examples include the North American craton during the Devono-Mississippian (Kominz and Bond, 1991) and the Australian craton during the Cenozoic (Lambeck, 1983).

TABLE 3
Mechanisms of continental epeirogeny

Mechanism	Scales			Reference
	Lateral (km)	Vertical (m)	Temporal (yr)	
Thermal Isostasy				
Thermal subsidence of rift margins	100–300	0–3000	10^7-10^8	Steckler & Watts, 1978; Royden & others, 1980
Mantle plumes	100–1000	0–3000	10^6-10^7	Griffiths & others, 1989; Westaway, 1993
Dynamic topography	500–5000	0–300[a]	10^7–10^8	Hager & others, 1985; Gurnis, 1990b, 1992a
Slabless windows	300–1000	0–2000	10^6–10^7	Crough & Thompson, 1977; Smith, 1982
Mantle upwelling owing to lithospheric delamination	100–1000	0–5000?	10^6–10^7?	Bird, 1978
Shear heating along lithosphere–asthenosphere interface	>10,000	0–3000?	10^7–10^8?	Melosh & Ebel, 1979
Partial crustal melting	100–1000	0–1000?	10^6–10^7?	McGetchin & others, 1980
Lower crustal magma intrusion	100–1000	0–3000?	10^6–10^7?	McKenzie, 1984
Lithospheric phase changes	1000–5000	0–1500?	10^7–10^8?	Smith, 1982
Non-thermal Isostasy				
Lithospheric flexure/glaciation	100–3000	0–1000	10^3–10^5	Peltier, 1980
Lithospheric flexure/tectonic loading	100–300	0–3000	10^6–10^7	Jordan, 1981; Quinlan & Beaumont, 1984
Lithospheric thickening/imbricate thrusting	100–1000	0–5000	10^6–10^8	Allègre & others, 1984; Molnar, 1989
Subducted slab buoyancy	100–1000	0–2000	10^6–10^8	Cross, 1986
Variations in intraplate stresses	100–1000	0–100	10^6–10^8?[b]	Gay, 1980; Cloetingh, 1988
Lithospheric underthrusting	100–1000	0–5000	10^6–10^8	Ni & Barazangi, 1983; Powell, 1986/87
Crustal denudation	100–1000	0–20?	$< 10^5$	Bishop & Brown, 1992
Subsurface dissolution	100–1000	0–100	10^4–10^6	Opdyke & others, 1984
Dynamic (Non-Isostatic)				
Viscous dynamic topography	200–1000	0–3000	10^7–10^8	Mitrovica & others, 1989; Gurnis, 1990a, 1992b

[a] Vertical offset in relation to center-of-Earth is 0–3000 m; value cited is in relation to hydrostatic geoid.
[b] Cathles & Hallam favor a shorter timescale: 10^4–10^6 yr.

5) *Lithospheric thickening owing to imbricate thrusting.* Overthrusting and complex deformation of continental margins under strong compressive regimes may result in lithospheric thickening over wide areas (Allègre and others, 1984). Thickening of the lithosphere underlying the Tibetan Plateau is probably due to complex internal structural displacements, although limited underthrusting of the margins of the Tibetan Plateau (ca. 50–80 km) by the Indian and Tarim Basin plates is likely (Hirn and others, 1984; Molnar, 1989). The degree of lithospheric thickening and scale of uplift is primarily a function of the rate of plate convergence (Molnar, 1989).

6) *Viscous dynamic topography.* Viscous coupling of subducting oceanic and overriding continental lithosphere may result in continental subsidence in back-arc settings (Hager, 1984; Mitrovica and others, 1989; Gurnis, 1992b). Changes in subduction rate and in the age and angle of penetration of subducting oceanic lithosphere result in variable crustal motions; generally, increased (decreased) subduction rates cause subsidence (uplift). This mechanism is of greatest potential significance during passive-to-active margin transitions, when onset of subduction may initiate back-arc subsidence (Gurnis, 1992b). A possible example is the Cretaceous-Tertiary epeirogenic history of western North America (Cross and Pilger, 1978; Mitrovica and others, 1989).

7) *Subducted slab buoyancy.* Subduction of young, hot oceanic lithosphere may result in shallowing subduction angles and physical buoyancy of adjacent continental margins (McGetchin and others, 1980; Cross, 1986). Progressive uplift may result when a subduction zone migrates toward a mid-ocean ridge. Tertiary uplift of the western margin of North America has been linked to approach of the East Pacific Rise (Cross, 1986).

8) *Slabless windows.* Collision of a mid-ocean ridge with a trench may produce a transform margin, along which spreading and formation of oceanic lithosphere cease and cratonward of which a hole develops in the subducting oceanic lithosphere. The progressively enlarging hole ("slabless window") permits advection of hot mantle material, resulting in thermal uplift of overlying continental lithosphere. High heat flow and uplift of the Basin and Range Province since the Early Miocene have been attributed to collision of North America with the East Pacific Rise and to development of a slabless window east of the San Andreas Fault Zone (Crough and Thompson, 1977).

3.2.3. Paleozoic Continental Epeirogeny

In analysis of paleo-continental epeirogeny, the temporal and spatial characteristics of the database of choice constrain the range of epeirogenic mechanisms about which inferences may be drawn. Epeirogenic histories reconstructed from continental flooding data at epochal intervals (as in this study) have a temporal resolution of $1–4 \times 10^7$ yr and a vertical resolution of 10 to 100 m (the latter a function of flooding data quality and resultant uncertainty ranges of elevation residuals; Fig. 10).

Because many epeirogenic mechanisms operate at similar length and time scales, it is generally not possible to identify the process responsible for a given crustal motion from these parameters alone. However, most types of epeirogenic motion have been shown to occur within specific plate tectonic contexts and, therefore, analysis of continental epeirogenic histories within a plate tectonic framework should lead to a better understanding of the origins of broad crustal motions. A complete analysis of this type is beyond the scope of the present paper, but the following discussion will serve to demonstrate the potential utility of linking paleo-continental epeirogenic and tectonic histories in order to constrain probable mechanisms of crustal motion. We will focus on Gondwana and Laurentia, touching only lightly on other Paleozoic continents:

Gondwana. Gondwanan elevation residuals suggest broad continental subsidence (−130 m) during the Early Silurian–Early Devonian and uplift (+260 m) during the Middle Devonian–Early Carboniferous (Fig. 10A). Siluro–Carboniferous epeirogeny may be related to the tectonic evolution of Gondwanan continental margins. Late Silurian–Early Devonian flooding of broad areas of South America, West Antarctica, and eastern Australia was followed by marine regression during the Middle Devonian–Early Carboniferous (Khain and Seslavinsky, 1991; Scotese and Golonka, 1993). In South America, where a widespread Late Devonian unconformity developed (Barrett and Isaacson, 1988), coeval arc-related magmatism and terrane accretion occurred along the southern Andean margin (Ramos and others, 1986). The Australian and Antarctic paleo-Pacific margins underwent a late Middle Devonian transition from transtensional to convergent active margins (Veevers, 1984), resulting in development of continental volcanic arc systems within the Lachlan Fold Belt of eastern Australia (Jell, 1988) and in North Victoria Land and Marie Byrd Land on the eastern Antarctic margin (Bradshaw and Webers, 1988).

An unusual aspect of the Gondwanan "epeirogenic" record is that major excursions are antithetic to coeval eustatic trends: 130-m subsidence in the Early Silurian–Early Devonian correlates with a 70-m sea-level fall, 260-m uplift in the Middle Devonian-Early Carboniferous with a 50-m sea-level rise, and 110-m subsidence in the Late Carboniferous with a 30-m sea-level fall (Figs. 9, 10). The large magnitude of these excursions and the 150-m.y. duration of the interval of covariance argues against a coincidental relationship and implies a strong causal connection between mid-Paleozoic eustasy and Gondwanan epeirogeny. One possibility is that faster MOR spreading rates caused both a global sea-level rise and uplift of Gondwanan continental margins owing to subduction of young oceanic lithosphere (e.g., Gurnis, 1992b) or continent-terrane collisions. Deceleration of MOR spreading rates in the mid-Carboniferous may be consistent with a major plate reorganization following collision of Laurussia and Gondwana, as evidenced by a mid-Carboniferous cusp in the North American APWP (DiVenere and Opdyke, 1991).

Laurentia. Laurentia/Laurussia exhibits sizable elevation residuals throughout the Paleozoic, implying large-scale subsidence during the Middle–Late Cambrian (−170 m), Late Ordovician (−140 m), and Middle-Late Devonian (−150 m), and uplift during the Early Ordovician (+100 m) and Early Silurian (+150 m;

and Trench, 1991; Cope and others, 1992). Thus, Middle-Late Cambrian uplift (+140 m) and Early–Late Ordovician subsidence (−170 m) may reflect syn-rift thermal doming and post-rift subsidence (Fig. 10D).

Siberia. Middle–Late Cambrian uplift (+150 m) may reflect collision and suturing of the Siberian craton with the Aldan and Barguzin terranes, and Late Devonian uplift (+60 m) may be related to the coeval Taimyr Orogeny in eastern Siberia (Fig. 10E; Zonenshain and others, 1990).

Kazakhstania. Owing to progressive assembly through accretion of a series of arcs and terranes around a microcontinental nucleus, Paleozoic Kazakhstania has a complex tectonic history (Zonenshain and others, 1990; Sengör and others, 1993). Late Carboniferous uplift (+140 m) was probably related to suturing of Kazakhstania with Laurussia and Siberia (Fig. 10F). Absence of coeval uplift of the latter two continents (Fig. 10B,E) is likely to have been a function of subduction zone polarity (Khain and Seslavinsky, 1991).

North China, South China, and Indochina. North China, South China, and Indochina fissioned sequentially from the Australian margin of Gondwana, probably during the Early–Middle Ordovician, Late Silurian–Early Devonian, and Siluro–Permian, respectively (Hutchison, 1989; Nie and others, 1990; Metcalfe, 1991). Late Ordovician uplift (+110 m) of the North China craton coincided with onset of dual-margin subduction along the Suolun–Xar Moron and Shanyang–Tongcheng tectonic zones (Fig. 10G; Wang, 1985). Early–Late Permian uplift of united China (+120 m) may have been linked to docking of North China with Siberia along the Suolun-Xar Moron suture (Wang, 1985; Nie and others, 1990).

Chukotka. Possible large-scale subsidence (−280 m) during the Late Ordovician–Late Silurian may record docking of Chukotka along the northern margin of North America, which culminated in the Late Silurian–Early Devonian Franklinian Orogeny (Fig. 10H). Docking occurred through sinistral oblique collision, which may have depressed the Chukotkan continental margin along a southward-dipping subduction zone (Trettin, 1989; Klaper, 1992).

This brief survey of the epeirogenic histories of Paleozoic continents suggests that most large elevation residuals may represent epeirogenic motions connected with major tectonic events. Although some elevation residual trends are consistent with known Paleozoic continental tectonic histories, as for Laurentia, others are enigmatic, such as the large mid-Paleozoic excursions exhibited by Gondwana. The range of mechanisms inferred for Paleozoic epeirogenic motions is nearly as broad as that documented for Cenozoic continents. Continued study of paleo-continental crustal motions within a plate tectonic context should provide new insights regarding mechanisms of continental epeirogeny.

4. Conclusions

Analysis of the flooding records of multiple, co-existing, tectonically-independent landmasses allows reconstruction of global sea-level trends and paleo-continental hypsometries and epeirogenic histories. The fundamental assumption underlying the method is that co-existing landmasses must have experienced the same range of eustatic fluctuations, and differences in degree of flooding therefore reflect

differences in continental coastal hypsometry. Patterns of hypsometric variation (i.e., similar hypsometric slopes but divergent inflection-point elevations) imply that epeirogenic motions are largely responsible for "hypsometric disequilibrium" among modern continents. Thus, continents may have stable long-term hypsometric profiles that are important controls on their flooding patterns, validating the reconstruction of paleo-continental hypsometric chords.

Scaling of paleo-continental elevations using Eurasian and American analogs yields mean Paleozoic sea-level estimates of +60 m and +160 m and sea-level elevation ranges of 24–102 m and 96–224 m, respectively. Choice of a Eurasian analog implies that modern eustatic elevations are rather typical for the Phanerozoic (modern sea level in an ice-free world +50 m), whereas choice of an American analog implies that they are unusualy low. Regardless of choice of analog, highstand elevations of +100 to +225 m are substantially lower than previous Paleozoic estimates of +300 m to +600 m but only slightly lower than estimates of +175 to +250 m for the Late Cretaceous highstand.

Differences between individual continental sea-level estimates and the global mean for each epoch are "elevation residuals" that represent either secular changes in paleo-continental hypsometry or errors in flooding estimates. Large elevation residuals are likely to have an epeirogenic origin, and many of these may be understood within the context of the tectonic history of individual continents. The most enigmatic continent is Gondwana, which exhibits large excursions in an antithetic sense to global sea-level trends during the Siluro–Carboniferous. This pattern requires a global control linking eustasy to epeirogeny, possibly via increased MOR spreading rates leading to uplift of Gondwanan continental margins through subduction of young oceanic lithosphere or continent-terrane collisions.

Acknowledgments

We would like to thank Bruce Wilkinson for considerable support and assistance during the early phases of this project, Robert Berner and Dave Osleger for helpful reviews, George Klein, Leigh Royden, and Dork Sahagian for commentary on a paper devoted to a related aspect of this project, and David Nash, Warren Huff, and Madeleine Briskin for stimulating discussions on this topic. Research support was provided by a University of Cincinnati Research Council grant and a Project Development Grant from the NAS National Research Council.

References

ALGEO, T. J., AND WILKINSON, B. H., 1991, Modern and ancient continental hypsometries: Journal of the Geological Society of London, v. 148, p. 643-654.

ALLÈGRE, C. J., AND 34 OTHERS, 1984, Structure and evolution of the Himalaya-Tibet orogenic belt: Nature, v. 307, p. 17-22.

ALLMENDINGER, R. W., 1986, Tectonic development, southeastern border of the Puna Plateau, northwestern Argentine Andes: Geological Society of America Bulletin, v. 97, p. 1070-1082.

BARRETT, S. F., AND ISAACSON, P. E., 1988, Devonian paleogeography of South America, in McMillan, N. J., Embry, A. F., and Glass, D. J., eds., Devonian of the World, Vol. 1: Regional Syntheses: Calgary, Canadian Society of Petroleum Geologists, p. 655-667.

BERNER, R. A., 1994, Geocarb II: a revised model of atmospheric CO2 over Phanerozoic time: American Journal of Science, v. 294, p. 56-91.

BIRD, P., 1978, Initiation of intracontinental subduction in the Himalaya: Journal of Geophysical Research, v. 83, p. 4975-4987.

BISHOP, P. AND BROWN, R., 1992, Denudational isostatic rebound of intraplate highlands: The Lachland River valley, Australia: Earth Surface Processes and Landforms, v. 17, p. 345-360.

BOND, G., 1976, Evidence for continental subsidence in North America during the Late Cretaceous global submergence: Geology, v. 4, p. 557-560.

BOND, G., 1978a, Evidence for Late Tertiary uplift of Africa relative to North America, South America, Australia and Europe: Journal of Geology, v. 86, p. 47-65.

BOND, G., 1978b, Speculations on real sea-level changes and vertical motions of continents at selected times in the Cretaceous and Tertiary Periods: Geology, v. 6, p. 247-250.

BOND, G. C., 1979, Evidence for some uplifts of large magnitude in continental platforms: Tectonophysics, v. 61, p. 285-305.

BOND, G. C., AND KOMINZ, M. A., 1991, Disentangling Middle Paleozoic sea level and tectonic events in cratonic margins and cratonic basins of North America: Journal of Geophysical Research, v. 96, no. B4, p. 6619-6639.

BOND, G. C., NICKERSON, P. A., AND KOMINZ, M. A., 1984, Breakup of a supercontinent between 625 Ma and 555 Ma: new evidence and implications for continental histories: Earth and Planetary Science Letters, v. 70, p. 325-345.

BOND, G. C., KOMINZ, M. A., GROTZINGER, J. P., AND STECKLER, M. S., 1989, Role of thermal subsidence, flexure and eustasy in the evolution of Early Paleozoic passive margin carbonate platforms, in Crevello, P., Wilson, J. L., Sarg, J. R., and Read, J. F., eds., Controls on Carbonate Platform and Basin Development: Society of Economic Paleontologists and Mineralogists Special Publication 44, p. 39-62.

BRADSHAW, M. A., AND WEBERS, G. F., 1988, The Devonian rocks of Antarctica, in McMillan, N. J., Embry, A. F., and Glass, D. J., eds., Devonian of the World, Vol. 1: Regional Syntheses: Calgary, Canadian Society of Petroleum Geologists, p. 783-795.

CATHLES, L. M., AND HALLAM, A., 1991, Stress-induced changes in plate density, Vail sequences, epeirogeny, and short-lived global sea level fluctuations: Tectonics, v. 10, p. 659-671.

CLOETINGH, S., 1988, Intraplate stresses: a tectonic cause for third-order cycles in apparent sea level?, in Wilgus, C. K., and others, eds., Sea-Level Changes: An Integrated Approach: Tulsa, Society of Economic Paleontologists and Mineralogists, Special Publication 42, p. 19-29.

COGLEY, J. G., 1985, Hypsometry of the continents: Zeitschrift fÿr Geomorphologie, Supplementband, v. 53.

COOK, T. D., AND BALLY, A.W., eds., 1975, Stratigraphic Atlas of North and Central America: Princeton, Princeton University Press, 272 p.

COPE, J. C. W., INGHAM, J. K., AND RAWSON, P. F., eds., 1992, Atlas of Palaeogeography and Lithofacies: London, Geological Society of London, Memoir 13, 153 p.

CROSS, T. A., AND PILGER, R. H., 1978, Tectonic controls of Late Cretaceous sedimentation, Western Interior, USA: Nature, v. 274, p. 653-657.

CROSS, T. A., 1986, Tectonic controls of foreland basin subsidence and Laramide style deformation, western United States, in Allen, P. A., and Homewood, P., eds., Foreland Basins: International Association of Sedimentologists, Special Publication 8, p. 15-40.

CROUGH, S. T., AND THOMPSON, G. A., 1977, Upper mantle origin of the Sierra Nevada uplift: Geology, v. 5, p. 396-399.

DALZIEL, I. W. D., 1992, Antarctica; a tale of two supercontinents?: Annual Review of Earth and Planetary Sciences, v. 20, p. 501-526.

DIVENERE, V. J., AND OPDYKE, N. D., 1991, Magnetic polarity stratigraphy and Carboniferous paleopole positions from the Joggins section, Cumberland structural basin, Nova Scotia: J. Geophysical Research, v. 96, p. 4051-4064.

DIXON, J., AND DIETRICH, J. R., 1990, Canadian Beaufort Sea and adjacent land areas, in Grantz, A., Johnson, L., and Sweeny, J. F., eds., The Arctic Ocean Region: Boulder, Colorado, Geological Society of America, The Geology of North America, vol. L, p. 239-256.

DONOVAN, D. T., AND JONES, E. J. W., 1979, Causes of world-wide changes in sea level: Journal of the Geological Society of London, v. 136, p. 187-192.

ENGEBRETSON, D. C., KELLEY, K. P., CASHMAN, H. J., AND RICHARDS, M. A., 1992, 180 million years of subduction: GSA Today, v. 2, p. 93-100 (not incl.).

FISCHER, A. G., 1984, The two Phanerozoic supercycles, in Berggren, W. A., and Van Couvering, J. A., eds., Catastrophes and Earth History: Princeton, Princeton University Press, p. 129-150.

FORSYTH, D. W., 1985, Subsurface loading and estimates of the flexural rigidity of continental lithosphere: Journal of Geophysical Research, v. 90, p. 12,623-12,632.

GAFFIN, S., 1987, Ridge volume dependence of seafloor generation rate and inversion using long term sealevel change: American Journal of Science, v. 287, p. 596-611.

GALER, S. J. G., 1991, Interrelationships between continental freeboard, tectonics and mantle temperature: Earth and Planetary Science Letters, v. 105, p. 214-228.

GAY, N. C., 1980, The state of stress in the plates, in Bally, A. W., Bender, P. L., McGetchin, T. R., and Walcott, R. I., eds., Dynamics of Plate Interiors: Washington, D.C., American Geophysical Union, Geodynamic Series 1, p. 145-153.

GRIFFITHS, R. W., GURNIS, M., AND EITELBERG, G., 1989, Holographic measurements of surface topography in laboratory models of mantle hotspots: Geophysical Journal, v. 96, p. 477-495.

GURNIS, M., 1988, Large-scale mantle convection and the aggregation and dispersal of supercontinents: Nature, v. 332, p. 695-699.

GURNIS, M., 1990a, Plate-mantle coupling and continental flooding: Geophysical Research Letters, v. 17, p. 623-626.

GURNIS, M., 1990b, Bounds on global dynamic topography from Phanerozoic flooding of continental platforms: Nature, v. 344, p. 754-756.

GURNIS, M., 1992a, Long-term controls on eustatic and epeirogenic motions by mantle convection: GSA Today, v. 2, p. 141-157 (not incl.).

GURNIS, M., 1992b, Rapid continental subsidence following the initiation and evolution of subduction: Science, v. 255, p. 1556-1558.

HAGER, B. H., 1984, Subducted slabs and the geoid: constraints on mantle rheology and flow: Journal of Geophysical Research, v. 89, p. 6003-6015.

HAGER, B., CLAYTON, R. W., RICHARDS, M. A., COMER, R. P., AND DZIEWONSKI, A. M., 1985, Lower mantle heterogeneity, dynamic topography and the geoid: Nature, v. 313, p. 541-545.

HALLAM, A., 1984, Pre-Quaternary sea-level changes: Annual Review of Earth and Planetary Science, v. 12, p. 205-243.

HAQ, B. U., HARDENBOL, J., AND VAIL, P. R., 1987, Chronology of fluctuating sea levels since the Triassic: Science, v. 235, p. 1156-1167.

HARLAND, W. B., ARMSTRONG, R. L., COX, A. V., CRAIG, L. E., SMITH, A. G., AND SMITH, D. G., 1990, A Geologic Time Scale 1989: Cambridge, Cambridge University Press, 263 p.

HARRISON, C. G. A., 1988, Eustasy and epeirogeny of continents on time scales between about 1 and 100 m.y.: Paleoceanography, v. 3, p. 671-684.

HARRISON, C. G. A., 1990, Long-term eustasy and epeirogeny in continents, in Revelle, R. R., and others, Sea-Level Change: Washington, D.C., National Academy Press, National Research Council, Studies in Geophysics, p. 141-158.

HARRISON, C. G. A., BRASS, G. W., SALTZMAN, E., SLOAN, J., II, SOUTHAM, J., AND WHITMAN, J. M., 1981, Sea level variations, global sedimentation rates and the hypsographic curve: Earth and Planetary Science Letters, v. 54, p. 1-16.

HARRISON, C. G. A., MISKELL, K. J., BRASS, G. W., SALTZMAN, E. S., AND SLOAN, J. L., II, 1983, Continental hypsography: Tectonics, v. 2, p. 357-377.

HARRISON, T. M., COPELAND, P., KIDD, W. S. F., AND YIN, A., 1992, Raising Tibet: Science, v. 255, p. 1663-1670.

HECKEL, P. H., 1986, Sea-level curve for Pennsylvanian eustatic marine transgressive-regressive depositional cycles along midcontinent outcrop belt, North America: Geology, v. 14, p. 330-334.

HELLER, P. L., AND ANGEVINE, C. L., 1985, Sea-level cycles during the growth of Atlantic-type oceans: Earth and Planetary Science Letters, v. 75, p. 417-426.

HELLER, P. L., WENTWORTH, C. M., AND POAG, C. W., 1982, Episodic post-rift subsidence of the United States Atlantic continental margin: Geological Society of America Bulletin, v. 93, p. 379-390.

HIRN, A., NERCESSIAN, A., SAPIN, M., JOBERT, G., XU, Z. X., GAO, E. Y., LU, D. Y., AND TENG, J. W., 1984, Lhasa block and bordering sutures–a continuation of a 500-km Moho traverse through Tibet: Nature, v. 307, p. 25-27.

HURST, J. M., McKERROW, W. S., SOPER, N. J., AND SURLYK, F., 1983, The relationship between Caledonian nappe tectonics and Silurian turbidite deposition in North Greenland: Journal of the Geological Society of London, v. 140, p. 123-131.

HUTCHISON, C. S., 1989, The Palaeo-Tethyan realm and Indosinian orogenic system of Southeast Asia, in Sengör, A.M.C., ed., Tectonic Evolution of the Tethyan Region: Dordrecht, Kluwer, p. 585-643.

JELL, J. S., 1988, Lower and Middle Devonian of Queensland, Australia, in McMillan, N. J., Embry, A. F., and Glass, D. J., eds., Devonian of the World, Vol. 1: Calgary, Canadian Society of Petroleum Geologists, p. 755-772.

JOHNSON, J. G., KLAPPER, G., AND SANDBERG, C. A., 1985, Devonian eustatic fluctuations in Euramerica: Geological Society of America Bulletin, v. 96, p. 567-587.

JOHNSON, M. E., BAARLI, B. G., NESTOR, H., RUBEL, M., AND WORSLEY, D., 1991, Eustatic sea-level patterns from the Lower Silurian (Llandovery Series) of southern Norway and Estonia: Geological Society of America Bulletin, v. 103, p. 315-335.

JORDAN, T. E., 1981, Thrust loads and foreland basin evolution, Cretaceous, western United States: American Association of Petroleum Geologists Bulletin, v. 65, p. 2506-2520.

KHAIN, V. E., AND SESLAVINSKY, K. B., 1991, Historical Geotectonics of the Paleozoic (in Russian): Moscow, Nedra, 398 p.

KING, L. C., 1962, The Morphology of the Earth: Edinburgh, Oliver and Boyd, 699 p.

KLAPER, E. M., 1992, The Paleozoic tectonic evolution of the northern edge of North America: A structural study of northern Ellesmere Island, Canadian Arctic Archipelago: Tectonics, v. 11, p. 854-870.

KOENEMANN, F. H., 1993, Tectonics of the Scandian Orogeny and the Western Gneiss Region in southern Norway: Geologische Rundschau, v. 82, p. 696-717.
KOMINZ, M. A., 1984, Oceanic ridge volumes and sea level change–an error analysis, in Schlee, J., ed., Interregional unconformities and hydrocarbon accumulation: American Association of Petroleum Geologists Memoir 36, p. 109-127.
KOMINZ, M. A., AND BOND, G. C., 1991, Unusually large subsidence and sea-level events during middle Paleozoic time: new evidence supporting mantle convection models for supercontinent assembly: Geology, v. 19, p. 56-60.
KUO, B.-Y., 1993, Thermal anomalies beneath the Australian-Antarctic discordance: Earth and Planetary Science Letters, v. 119, p. 349-364.
LAMBECK, K., 1983, The role of compressive forces in intracratonic basin formation and mid-plate orogenies: Geophysical Research Letters, v. 10, p. 845-848.
LARSON, R. L., 1991, Latest pulse of the Earth: Evidence for a mid-Cretaceous superplume: Geology, v. 19, p. 547-550.
LEVY, M., AND CHRISTIE-BLICK, N., 1991, Tectonic subsidence of the early Paleozoic passive continental margin in eastern California and southern Nevada: Geological Society of America Bulletin, v. 103, p. 1590-1606.
LINDSAY, J. F., AND KORSCH, R. J., 1989, Interplay of tectonics and sea-level changes in basin evolution: an example from the intracratonic Amadeus Basin, central Australia: Basin Research, v. 2, p. 3-25.
McGETCHIN, T. R., BURKE, K. C., THOMPSON, G. A., AND YOUNG, R. A., 1980, Mode and mechanisms of plateau uplifts, in Bally, A. W., Bender, P. L., McGetchin, T. R., and Walcott, R. I., eds., Dynamics of Plate Interiors: Washington, D.C., American Geophysical Union, Geodynamic Series 1, p. 99-110.
McKENZIE, D., 1984, A possible mechanism for epeirogenic uplift: Nature, v. 307, p. 616-618.
McKERROW, W. S., SCOTESE, C. R., AND BRASIER, M. D., 1992, Early Cambrian continental reconstructions: Journal of the Geological Society of London, v. 149, p. 599-606.
MELOSH, H. J., AND EBEL, J., 1979, A simple model for thermal instability in the asthenosphere: Geophysical Journal of the Royal Astronomical Society, v. 59, p. 419-436.
METCALFE, I., 1991, Late Palaeozoic and Mesozoic palaeogeography of Southeast Asia: Palaeogeography, Palaeoclimatology, Palaeoecology, v. 87, p. 211-221.
MITROVICA, J. X., BEAUMONT, C., AND JARVIS, G. T., 1989, Tilting of continental interiors by the dynamical effects of subduction: Tectonics, v. 8, p. 1079-1094.
MOLNAR, P., 1989, The geological evolution of the Tibetan Plateau: American Scientist, v. 77, p. 350-360.
MOORES, E. M., 1991, The Southwest U.S.-East Antarctic (SWEAT) connection: a hypothesis: Geology, v. 19, p. 425-428.
MÖRNER, N.-A., 1976, Eustasy and geoid changes: Journal of Geology, v. 84, p. 123-151.
NI, J., AND BARAZANGI, M., 1983, High-frequency seismic wave propagation beneath the Indian Shield, Himalayan arc, Tibetan Plateau, and surrounding regions: high uppermost mantle velocities and efficient Sn propagation beneath Tibet: Geophysical J. Royal Astronomical Society, v. 72, p. 665-689.
NIE, S.-Y., ROWLEY, D. B., AND ZIEGLER, A. M., 1990, Constraints on the locations of Asian microcontinents in Palaeo-Tethys during the Late Palaeozoic, in McKerrow, W. S., and Scotese, C. R., eds., Palaeozoic Palaeogeography and Biogeography: Geological Society of London Memoir 12, p. 397-409.
OLDOW, J. S., BALLY, A. W., LALLEMANT, H. G. A., AND LEEMAN, W. P., 1989, Phanerozoic evolution of the North American Cordillera; United States and Canada, in

Bally, A. W., and Palmer, A. R., editors, The Geology of North America–An overview: Boulder, Colorado, Geological Society of America, The Geology of North America, vol. A, p. 139-232.

OPDYKE, N. D., SPANGLER, D. P., SMITH, D. L., JONES, D. S., AND LINDQUIST, R. C., 1984, Origin of the epeirogenic uplift of Pliocene-Pleistocene beach ridges in Florida and development of the Florida karst: Geology, v. 12, p. 226-228.

OSLEGER, D., AND READ, J. F., 1993, Comparative analysis of methods used to define eustatic variations in outcrop: Late Cambrian interbasinal sequence development: American Journal of Science, v. 293, p. 157-216.

Paleogeographic Atlas of Australia, Vol. 1–Cambrian, 1988: Canberra, Australian Government Publishing Service.

Paleogeographic Atlas of Australia, Vol. 2–Ordovician, 1992: Canberra, Australian Government Publishing Service.

PALMER, J., SEMPÉRÉ, J. C., CHRISTIE, D., AND PHIPPS MORGAN, J., 1993, Morphology and tectonics of the Australian-Antarctic Discordance between 123E and 128E: Marine Geophysical Research, v. 15, p. 21-152.

PEATE, D. W., HAWKESWORTH, C. J., MANTOVANI, M. S. M., AND SHUKOWSKY, W., 1990, Mantle plumes and flood-basalt stratigraphy in the ParanÛ, South America: Geology, v. 18, p. 1223-1226.

PELTIER, W. R., 1980, Models of glacial isostasy and relative sea level, in Bally, A. W., Bender, P. L., McGetchin, T. R., and Walcott, R. I., eds., Dynamics of Plate Interiors: Washington, D.C., American Geophysical Union, Geodynamic Series 1, p. 111-128.

PITMAN, W. C., III, 1978, Relationship between eustacy and stratigraphic sequences of passive margins: Geological Society of America Bulletin, v. 89, p. 1389-1403.

POWELL, C.McA., 1986/87, Continental underplating model for the rise of the Tibetan Plateau: Earth and Planetary Science Letters, v. 81, p. 79-94.

PYLE, D. G., CHRISTIE, D. M., AND MAHONEY, J. J., 1992, Resolving an isotopic boundary within the Australian-Antarctic Discordance: Earth and Planetary Science Letters, v. 112, p. 161-178.

QUINLAN, G. M., AND BEAUMONT, C., 1984, Appalachian thrusting, lithospheric flexure, and the Paleozoic stratigraphy of the eastern interior of North America: Canadian Journal of Earth Sciences, v. 21, p. 973-996.

RAMOS, V. A., JORDAN, T. E., ALLMENDINGER, R. W., MPODOZIS, C., KAY, S. M., CORTES, J. M., AND PALMA, M., 1986, Paleozoic terranes of the central Argentine-Chilean Andes: Tectonics, v. 5, p. 855-880.

RIDING, R., 1984, Sea-level changes and the evolution of benthic marine calcareous algae during the Palaeozoic: Journal of the Geological Society of London, v. 141, p. 547-553.

ROBARDET, M., PARIS, F., AND RACHEBOEUF, P. R., 1990, Palaeogeographic evolution of southwestern Europe during Early Palaeozoic times, in McKerrow, W. S., and Scotese, C. R., eds., Palaeozoic Palaeogeography and Biogeography: Geological Society of London Memoir 12, p. 411-419.

RONOV, A. B., 1980, The Earth's sedimentary shell (Quantitative patterns of its structures, compositions and evolution), in Yaroshevsky, ed., The Earth's Sedimentary Shell (Quantitative patterns of its structures, compositions and evolution): Moscow, Nauka, p. 1-80; also, American Geological Institute Reprint Series, v. 5, p. 1-73, 1983.

RONOV, A. B., 1994, Phanerozoic transgressions and regressions on the continents: a quantitative approach based on areas flooded by the sea and areas of marine and continental deposition: American Journal of Science, v. 294, p. 777-801.

RONOV, A. B., KHAIN, V. E., BALUKHOVSKY, A. N., AND SESLAVINSKY, K. B., 1980, Quantitative analysis of Phanerozoic sedimentation: Sedimentary Geology, v. 25, p. 311-325.

RONOV, A. B., KHAIN, V. E., AND SESLAVINSKY, K. B., 1984, Atlas of Lithologic-Paleogeographic Maps of the World--Late Precambrian and Paleozoic of Continents (in Russian): Leningrad, 70 p.

ROSENDAHL, B. R., 1987, Architecture of continental rifts with special reference to East Africa: Annual Review of Earth and Planetary Sciences, v. 15, p. 445-503.

ROYDEN, L., SCLATER, J. G., AND VON HERZEN, R. P., 1980, Continental margin subsidence and heat flow: important parameters in formation of petroleum hydrocarbons: American Association of Petroleum Geologists Bulletin, v. 64, p. 173-187.

RUDDIMAN, W.F., PRELL, W.L., AND RAYMO, M.E., 1989, Late Cenozoic uplift in southern Asia and the American West: rationale for general circulation modeling experiments: Journal of Geophysical Research, v. 94, p. 18,379-18,391.

SAHAGIAN, D., 1987, Epeirogeny and eustatic sea level as inferred from Cretaceous shoreline deposits: applications to the central and western United States: Journal of Geophysical Research, v. 92, p. 4895-4904.

SAHAGIAN, D., 1988, Epeirogenic motions of Africa as inferred from Cretaceous shoreline deposits: Tectonics, v. 7, p. 125-138.

SAHAGIAN, D., 1989, Epeirogeny of Europe and western Asia: Cretaceous Research, v. 10, p. 33-48.

SCHENK, P. E., 1991, Events and sea-level changes on Gondwana's margin: the Meguma Zone (Cambrian to Devonian) of Nova Scotia, Canada: Geological Society of America Bulletin, v. 103, p. 512-521.

SCOTESE, C. R., AND GOLONKA, J., 1993, PALEOMAP Paleogeographic Atlas: Department of Geology, University of Texas, Arlington, 35 p.

SCOTESE, C. R., AND McKERROW, W. S., 1990, Revised World maps and introduction, in McKerrow, W. S., and Scotese, C. R., eds., Palaeozoic Palaeogeography and Biogeography: Geological Society of London Memoir 12, p. 1-21.

SCOTESE, C. R., BAMBACH, R. K., BARTON, C., VAN DER VOO, R., AND ZIEGLER, A. M., 1979, Paleozoic base maps: Journal of Geology, v. 87, p. 217-277.

SEMPÉRÉ, J.-C., PALMER, J., CHRISTIE, D. M., MORGAN, J. P., AND SHOR, A. N., 1991, Australian-Antarctic discordance: Geology, v. 19, p. 429-432.

SENGÖR, A. M. C., NATAL'IN, B. A., AND BURTMAN, V. S., 1993, Evolution of the Altaid tectonic collage and Palaeozoic crustal growth in Eurasia: Nature, v. 364, p. 299-307.

SESLAVINSKY, K. B., 1987, Sedimentation and volcanism during the Caledonian stage of Earth history (in Russian): Moscow, Nedra, 192 p.

SESLAVINSKY, K. B., 1991, Global transgressions and regressions of the Paleozoic (in Russian): Izvestia of the U.S.S.R. Academy of Sciences, Geological Series, No. 1, p. 71-79; English translation: International Geological Review, v. 2, p. 3-11.

SMITH, A. G., 1982, Late Cenozoic uplift of stable continents in a reference frame fixed to South America: Nature, v. 296, p. 400-404.

STECKLER, M. S., AND WATTS, A. B., 1978, Subsidence of the Atlantic-type continental margin off New York: Earth and Planetary Science Letters, v. 41, p. 1-13.

STERN, T. A., AND HOLT, W. E., 1994, Platform subsidence behind an active subduction zone: Nature, v. 368, p. 233-236.

TORSVIK, T. H., AND TRENCH, A., 1991, The Ordovician history of the Iapetus ocean in Britain: new palaeomagnetic constraints: Journal of the Geological Society of London, v. 148, p. 423-425.

TORSVIK, T. H., RYAN, P. D., TRENCH, A., AND HARPER, D. A. T., 1991, Cambrian-Ordovician paleogeography of Baltica: Geology, v. 19, p. 7-10.

TORSVIK, T. H., SMETHURST, M. A., VAN DER VOO, R., TRENCH, A., ABRAHAMSEN, N., AND HALVORSEN, E., 1992, Baltica: a synopsis of Vendian-Permian

palaeomagnetic data and their palaeotectonic implications: Earth-Science Reviews, v. 33, p. 133-152.

TRETTIN, H. P., 1989, The Arctic Islands, in Bally, A. W., and Palmer, A. R., eds., The Geology of North America–An Overview: Boulder, Colorado, Geological Society of America, The Geology of North America, v. A, p. 349-370.

TURCOTTE, D. L., AND BURKE, K., 1978, Global sea-level changes and the thermal structure of the Earth: Earth and Planetary Science Letters, v. 41, p. 341-346.

VAIL, P. R., MITCHUM, R. M., JR., AND THOMPSON, S., III, 1977, Global cycles of relative changes of sea level, in Payton, C. E., ed., Seismic Stratigraphy and Global Changes of Sea Level: Tulsa, American Association of Petroleum Geologists Memoir 26, p. 83-97.

VEEVERS, J. J., ed., 1984, Phanerozoic Earth history of Australia: Oxford, Clarendon, 418 p.

WANG, H.-Z., comp., 1985, Atlas of the Palaeogeography of China: Beijing, Cartographic Publishing House, 143 maps + 28 p.

WESTAWAY, R., 1993, Forces associated with mantle plumes: Earth and Planetary Science Letters, v. 119, p. 331-348.

WHITE, R. S., AND McKENZIE, D. P., 1989, Magmatism at rift zones: the generation of volcanic continental margins and flood basalts: Journal of Geophysical Research, v. 94, p. 7685-7729.

WILKINSON, B. H., AND GIVEN, R. K., 1986, Secular variation in abiotic marine carbonates: Constraints on Phanerozoic atmospheric carbon dioxide contents and oceanic Mg/Ca ratios: Journal of Geology, v. 94, p. 321-333.

WILKINSON, B. H., OWEN, R. M., AND CARROLL, A. R., 1985, Submarine hydrothermal weathering, global eustasy, and carbonate polymorphism in Phanerozoic marine oolites: Journal of Sedimentary Petrology, v. 55, p. 171-183.

WISE, D. U., 1974, Continental margins, freeboard and the volumes of continents and oceans through time, in Burk, C. A., and Drake, C. L., editors, The Geology of Continental Margins: New York, Springer, p. 45-58.

WORSLEY, T. R., NANCE, D., AND MOODY, J. B., 1984, Global tectonics and eustasy for the past 2 billion years: Marine Geology, v. 58, p. 373-400.

WYATT, A. R., 1986, Post-Triassic continental hypsometry and sea level: Journal of the Geological Society of London, v. 143, p. 907-910.

WYATT, A. R., 1987, Shallow water areas in space and time: Journal of the Geological Society of London, v. 144, p. 115-120.

ZIEGLER, P. A., 1989, Evolution of Laurussia: Dordrecht, Kluwer, 102 p.

ZONENSHAIN, L. P., KUZMIN, M. I., AND KONONOV, M. V., 1987, Absolute reconstructions of the state of continents in Paleozoic and Early Mesozoic: Geotectonics, v. 21, p. 199-212.

ZONENSHAIN, L. P., KUZMIN, M. I., AND NATAPOV, L. M. (Page, B. M., ed.), 1990, Geology of the USSR: A Plate-Tectonic Synthesis, Geodynamics Series 21: Washington, D.C., American Geophysical Union, 242 p.